

Quantifying disparities in intimate partner violence: a machine learning method to correct for underreporting

Divya Shanmugam^{1,5}, Kaihua Hou², and Emma Pierson^{3,4}

¹ Department of Electrical Engineering and Computer Science, MIT, Cambridge, MA 02139, USA

² Malone Center of Engineering in Healthcare, Johns Hopkins University School of Medicine, Baltimore, Maryland

³ Department of Computer Science, Cornell Tech, New York, NY 10044, USA

⁴ Department of Population Health Sciences, Weill Cornell Medical College, New York, NY 10021, USA

⁵ Indicates corresponding author. Please address all correspondence to divyas@mit.edu.

Abstract

The first step towards reducing the pervasive disparities in women’s health is to quantify them. Accurate estimates of the *relative prevalence* across groups — capturing, for example, that a condition affects Black women more frequently than white women — facilitate effective and equitable health policy which prioritizes groups who are disproportionately affected by a condition. However, it is difficult to estimate relative prevalence when a health condition is underreported, as many women’s health conditions are. In this work, we present PURPLE, a method for accurately estimating the relative prevalence of underreported health conditions which builds upon the positive unlabeled machine learning framework. We show that under a commonly made assumption—that the probability of having a health condition given a set of symptoms remains constant across groups—we can recover the relative prevalence, even without restrictive assumptions commonly made in positive unlabeled learning and even if it is impossible to recover the absolute prevalence. We conduct experiments on synthetic and real health data which demonstrate PURPLE’s ability to recover the relative prevalence more accurately than do previous methods. We then use PURPLE to quantify the relative prevalence of intimate partner violence (IPV) in two large emergency department datasets. We find higher prevalences of IPV among patients who are on Medicaid, not legally married, in lower-income zipcodes, in metropolitan counties, and non-white. We show that correcting for underreporting is important to accurately quantify these disparities, and that failing to do so yields less plausible estimates. Our method is broadly applicable to underreported conditions in women’s health, as well as to gender biases beyond healthcare.

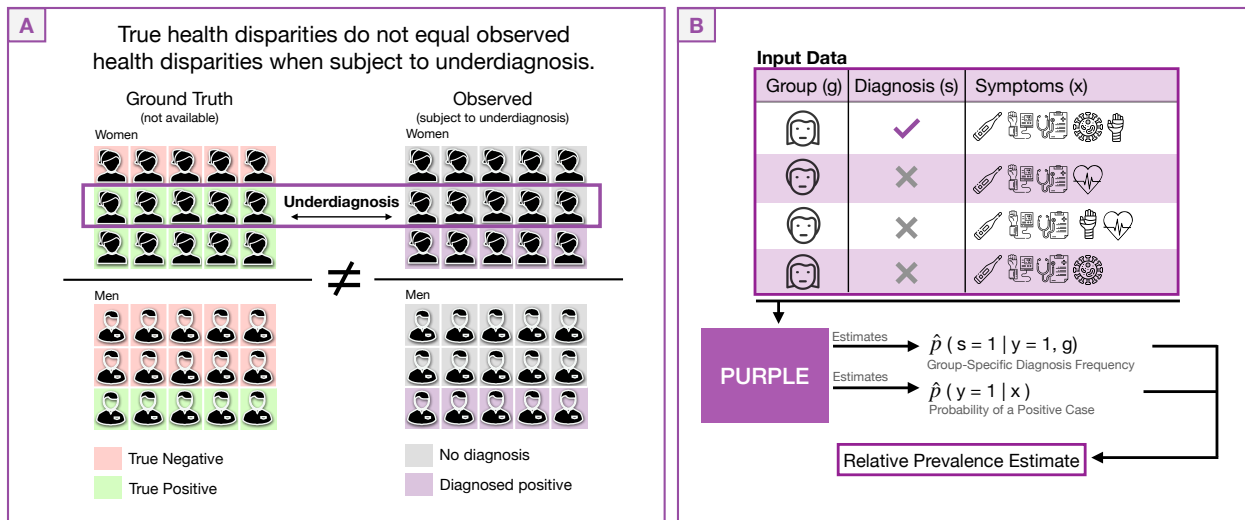


Figure 1: Underreporting can skew observed relative prevalences and conceal health disparities. PURPLE is designed to estimate the relative prevalence while correcting for underreporting. A) Underreporting leads to inaccurate observed relative prevalences. Understanding the relative prevalence of a health condition between groups g —for example, men and women—is important to effective medical care. However, these estimates are often based on diagnoses s (i.e. a diagnosed positive or no diagnosis) instead of the true patient state y (sick vs. not sick). Underreporting, which is known to vary by demographic groups, leads to inaccurate relative prevalence estimates that can hide the groups most affected by a condition. **B) PURPLE uses data on patient diagnoses s , symptoms x , and group membership g to accurately estimate the relative prevalence of a condition.** PURPLE first estimates the group-specific diagnosis probability, $p(s = 1 | y = 1, g)$, and disease likelihood, $p(y = 1 | x)$, up to constant multiplicative factors, and then combines these estimates to compute the relative prevalence. We show this is possible under three widely-made assumptions: no false positives, random diagnosis within groups, and constant $p(y = 1 | x)$ between groups.

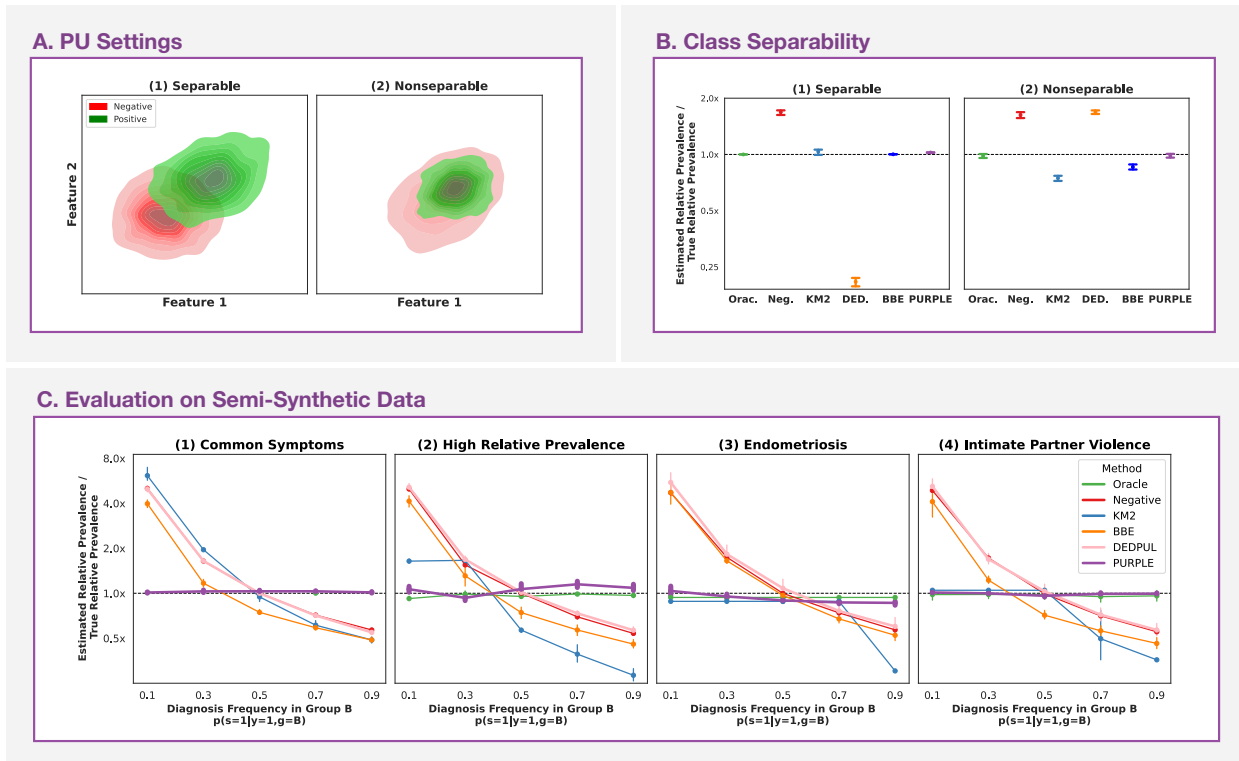


Figure 2: Validation of PURPLE on synthetic and semi-synthetic data. **A) Methods in positive-unlabeled learning commonly make assumptions about the separability of the positive and negative distributions.** Settings in which underreporting occurs map directly to work in positive-unlabeled learning, in which learning algorithms have access to a set of positive labeled examples and an unlabeled mixture of positive and negative examples. Most works in positive-unlabeled learning assume A (left panel), or a positive subdomain, while no method can accommodate the distributions pictured in the right panel. PURPLE makes no assumptions about the separability of the positive and negative distributions, and instead assumes that $p(y = 1|x)$ remains constant across patient subgroups. **B) PURPLE accurately recovers the relative prevalence on both separable and nonseparable synthetic data.** The vertical axis plots the ratio of estimated relative prevalence to true relative prevalence, with 1 (dotted line) indicating perfect performance. We report variation across 5 randomized train, validation and test splits. *Negative*, *KM2*, *BBE*, and *DEDPUL* baselines do not always accurately estimate the relative prevalence, especially on nonseparable data. *Oracle* is impossible to implement in practice because it relies on ground truth labels y which are not available; it is provided as a metric for ideal performance. **C) PURPLE recovers the relative prevalence accurately in simulations based on real health data.** We generate semi-synthetic data by using patient visits from MIMIC-IV¹ and simulating a disease label given a set of symptoms. This allows us to test PURPLE on a real, high-dimensional distribution of symptoms while retaining access to ground truth labels. Each dataset simulates disease likelihood on the basis of a different symptom set: **(1)** symptoms that appear most frequently, **(2)** symptoms which occur frequently in one group but not the other, **(3)** symptoms that co-occur frequently with endometriosis, and **(4)** symptoms known to indicate risk of intimate partner violence based on past literature. We define group A to be Black patients, and group B to be white patients. Across symptom sets, and a range of group-specific diagnosis frequencies, PURPLE produces more consistently accurate relative prevalence estimates than existing work. Two semisynthetic experiments involving real conditions in women’s health—endometriosis and intimate partner violence—demonstrate the potential to apply PURPLE to conditions in women’s health and produce accurate, actionable relative prevalence estimates.

Relative Prevalence of Intimate Partner Violence

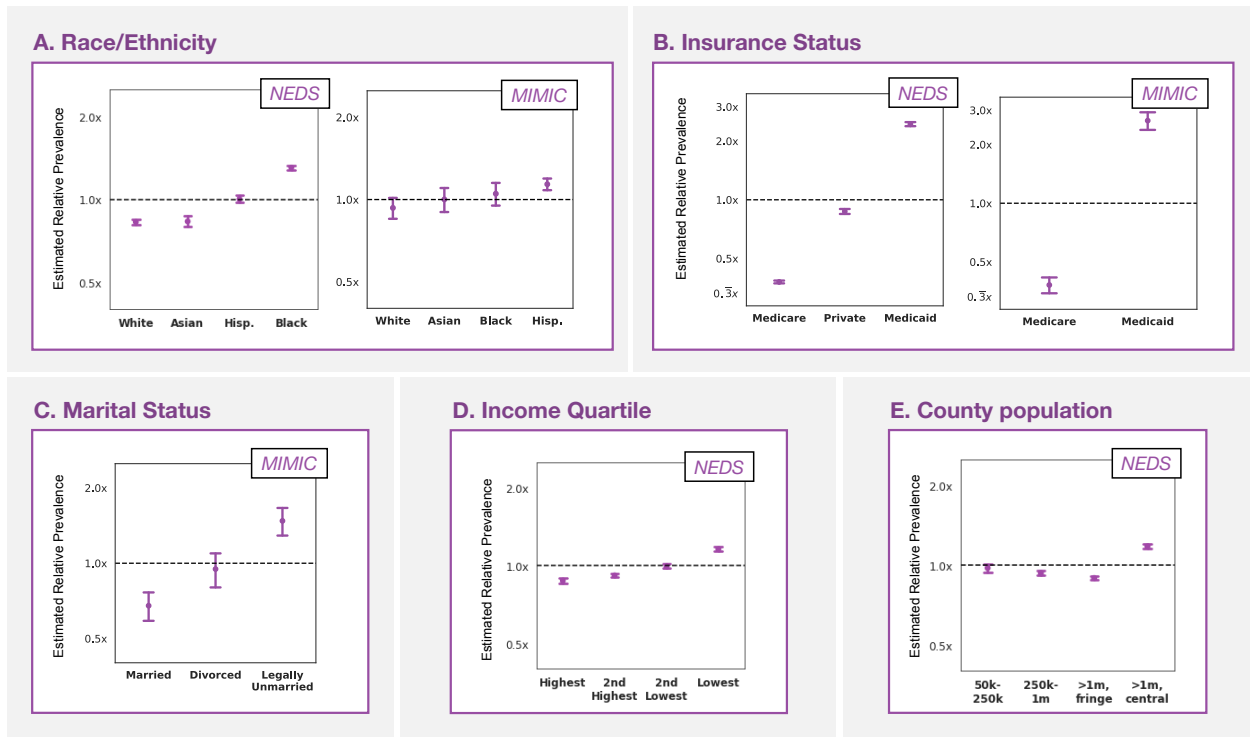


Figure 3: Estimates of the relative prevalence of intimate partner violence across demographic subgroups. We apply PURPLE to two large emergency department datasets: NEDS² and MIMIC-IV³. We compute each relative prevalence with respect to each group’s complement (i.e. estimating the prevalence of IPV among married patients vs. non-married patients). Relative prevalences are higher among non-white patients overall (A) though these disparities are noisily estimated in the MIMIC dataset and the ordering across race groups is not completely consistent. We also find higher prevalences among patients who are on Medicaid (B), not legally married (C), in lower-income zipcodes (D), and in metropolitan counties (E). Counties with more than 1 million residents are further differentiated by how urban they are (as “central” or “fringe”). Error bars report the standard deviations for each estimate across 5 randomized train/test splits of each dataset. Panels C, D, and E are reported on only a single dataset due to different demographic feature availability in the two datasets; note the slightly larger y-axis range on Panel B due to the greater range of the estimates.

Introduction

There are enormous disparities in women’s health across race, age, socioeconomic status, and other dimensions. Mitigating these disparities requires accurate estimates of the extent to which a medical condition disproportionately affects different groups. The *relative prevalence* does so by capturing how much more frequently a condition occurs in one group compared to another — $\frac{\text{prevalence in group A}}{\text{prevalence in group B}}$ — with high relative prevalence estimates suggesting concrete areas to increase funding, research, and resources. Public health decisions often rely on such estimates to develop, allocate, and advocate for interventions. For example, research revealing startling disparities in maternal mortality between Black and white women⁴ led to Congressional policy that has invested billions in funding towards evidence-based interventions to improve Black maternal health⁵.

However, it remains challenging to produce accurate relative prevalence estimates for many conditions in women’s health due to widespread *underreporting* (Fig. 1A). With underreported health conditions, only a small percentage of true positives may be labeled as positive; worse, the probability of correctly diagnosing a positive case can vary by group⁶. This is especially relevant to intimate partner violence, a notoriously underreported condition: true cases are only correctly diagnosed an estimated $\sim 25\%$ of the time, and this probability varies across racial groups⁷. Underreporting in one group and not another can mask health disparities, making it appear that a condition is equally prevalent in two populations when it is not, or more prevalent in one population than in another when it is not. These errors obscure where resources are most needed, and consequently inhibit the development of effective health policy.

Efforts in both epidemiology and machine learning have addressed these challenges, but often rely on either data which is unavailable, or assumptions which are unrealistic in women’s health contexts (refer to Sec. S1 for a detailed discussion of related work). Epidemiological work attempts to quantify true prevalences in the context of imperfect diagnostic tests, and commonly assumes the presence of information which is not always available (for example, ground truth annotations^{8–12}, multiple tests^{13–15}, or informative priors¹⁶). For conditions in women’s health, we often have no

access to ground truth, only a single diagnosis per patient, and no notion of how accurate that diagnosis truly is. The machine learning literature has modeled underreporting using the positive-unlabeled (PU) learning framework, which assumes that only some positive cases are correctly labeled as positive, and the unlabeled examples consist of both true negatives and unlabeled true positives. In order to recover prevalence in the presence of underdiagnosis, many PU learning methods assume that there is a region of the feature space where cases are certain to be true positives. However, this is a restrictive assumption which, while potentially suitable in other PU settings, is unlikely to hold in health data¹⁷ because it is rare that a set of symptoms corresponds to a health condition with 100% certainty. This is especially true in the context of intimate partner violence, where symptoms are frequently not specific to a particular condition (for example, pregnancy complications, which are well-known to occur at higher rates among IPV patients¹⁸, could suggest a number of underlying conditions, rather than just one).

Here, we present **PURPLE** (**P**ositive **U**nabeled **R**elative **P**revalence **E**stimator), a method that is complementary to the epidemiology and PU learning literature. In contrast to epidemiological approaches, it requires no external information (for example, the sensitivity and specificity of a test) to recover the relative prevalence of an underreported disease. In contrast to the PU learning literature, **PURPLE** relies on no assumptions about the symptom distributions of positive and negative cases. **PURPLE** is designed to address underreporting in intimate partner violence, and women’s health more broadly, by estimating the relative prevalence of the condition given three assumptions: 1) no false positive diagnoses; 2) random diagnosis within group; and 3) constant $p(y = 1|x)$ between groups, i.e., that the probability of having a disease conditional on symptoms remains constant across groups. The first two assumptions are standard in PU learning; the third, which is specific to our method, replaces PU assumptions about the separability of the positive and negative classes. We show that if these assumptions are satisfied, it is possible to recover the relative prevalence even if it is not possible to recover the absolute prevalence: that is, $\frac{\text{prevalence in group A}}{\text{prevalence in group B}}$ can be estimated even if neither the numerator nor denominator can. **PURPLE** does this by jointly estimating the conditional probability that a case is a true positive given a set of symptoms, and

the diagnosis probability (i.e., the probability a positive case is diagnosed as such; Fig. 1B). We demonstrate via experiments on synthetic and real health data that PURPLE recovers the relative prevalence more accurately than do existing methods. We provide methods for checking whether PURPLE’s underlying assumptions hold, and show that even under a plausible violation of the assumptions PURPLE still provides a useful lower bound on the magnitude of disparities.

Having validated PURPLE, we use it to estimate the relative prevalence of the condition which motivates this work — intimate partner violence (IPV) — in two widely-used datasets of electronic health records, which together describe millions of emergency department visits: MIMIC-IV³ and NEDS². Across both datasets, we find higher prevalences of IPV among patients who are on Medicaid than among those on Medicare. Relative prevalences are higher among non-white patients (though these disparities are noisily estimated in the MIMIC dataset). We also quantify the relative prevalence of IPV across income quartiles, marital statuses, and the rural-urban spectrum, finding that IPV is more prevalent among patients who are lower-income, not legally married, and in metropolitan counties. Finally, we show that PURPLE’s corrections for underreporting are important: they yield more plausible estimates of how relative prevalence varies with income than estimation methods which do not correct for underreporting. Specifically, PURPLE estimates that the relative prevalence of IPV decreases with income, consistent with prior work^{19–21}. In contrast, failing to correct for underdiagnosis (i.e. computing relative prevalence estimates using observed diagnoses) yields estimates which do not show any consistent trend with respect to income, and which are harder to explain. Overall, this analysis contributes to the literature on IPV disparities in several ways: it uses some of the largest and most recent samples; evaluates robustness across multiple datasets; and corrects for underreporting.

Together, our analyses illustrate how PURPLE is a general method for estimating relative prevalences in the presence of underreporting, allowing practitioners to discover and quantify group-specific disparities in a wide range of settings in women’s health and beyond.

Results

Here, we introduce PURPLE, a method to quantify disparities in prevalence of a health condition between groups given only positive and unlabeled data. A key idea underpinning our method is that knowing the exact prevalence in a group is not necessary to calculate the *relative* prevalence across groups: one can estimate the fraction $\frac{\text{prevalence in group A}}{\text{prevalence in group B}}$ without knowing its numerator or denominator. We adopt terminology standard in the PU learning literature and assume that we have access to three pieces of data for the i th example: a feature vector x_i ; a group variable g_i ; and a binary observed label s_i . We let y_i denote the true (unobserved) label. In healthcare, example i may correspond to a specific patient and their presenting symptoms (x_i), race (g_i), and observed diagnosis (s_i). Here, y_i corresponds to whether the patient truly *has* the medical condition. We first introduce PURPLE and then validate our approach on synthetic and semi-synthetic data.

Overview of PURPLE: Positive-Unlabeled Relative Prevalence Estimation

We provide a conceptual overview of PURPLE here and describe the full details in Sections M1.2-M1.4. PURPLE is designed to address how, for underreported women’s health conditions, the ratio of *diagnosis rates* between demographic groups may not equal the ratio of *true prevalences*, due to differential underreporting across groups. To address this, PURPLE first uses the observed data to learn a model of which symptoms correlate with having the condition; so long this relationship between symptoms and the condition remains constant across groups, we will be able to estimate the relative prevalence. Mathematically, PURPLE first estimates $p(y = 1|x)$ up to a constant multiplicative factor; second, it uses this estimate to compute the relative prevalence between groups. We use p to denote the true probabilities in the underlying data distribution and \hat{p} to denote PURPLE’s estimates of these probabilities.

1. **Estimate $p(y = 1|x)$ up to a constant factor.** PURPLE fits the following model:

$$\underbrace{\hat{p}(s = 1|g, x)}_{\text{probability patient is diagnosed}} = \underbrace{\hat{p}(y = 1|x)}_{\text{probability patient truly has condition}} \cdot \underbrace{\hat{p}(s = 1|y = 1, g)}_{\text{probability true positives are correctly diagnosed}} \quad (1)$$

In other words, PURPLE models the probability a patient is diagnosed with a condition as the

product of two terms: the probability the patient truly has the condition, and the probability that true positives are correctly diagnosed. The first term is constant across groups g while the second can vary, accounting for underdiagnosis. This decomposition is valid under three assumptions which we discuss below. To estimate the two terms on the right hand side of Equation 1, we parameterize the first term as a single-layer neural network and the second as a constant $c_g \in [0, 1]$ for each group g . We optimize these parameters by minimizing the cross-entropy loss between the predicted $\hat{p}(s = 1|g, x)$ and the true $p(s = 1|g, x)$, which is possible because s, g , and x are all observed (Sec. M1.4). Note that we can only estimate both terms on the right hand side up to a constant multiplicative factor, because multiplying the first term by a non-negative β and dividing the second term by β leaves $\hat{p}(s = 1|g, x)$ unchanged.

2. **Estimate the relative prevalence using $\hat{p}(y = 1|x)$.** Fortunately, even though $\hat{p}(y = 1|x)$ is only correct up to a constant multiplicative factor, this suffices to estimate the relative prevalence $\frac{p(y=1|g=a)}{p(y=1|g=b)}$, as we derive in Sec. M1.2. Specifically, our estimator of the relative prevalence is

$$\frac{\sum_x \hat{p}(y = 1|x) \hat{p}(x|g = a)}{\sum_x \hat{p}(y = 1|x) \hat{p}(x|g = b)} \quad (2)$$

In practice, this is simply the mean value of $\hat{p}(y = 1|x)$ for samples from group a divided by the mean value of $\hat{p}(y = 1|x)$ for samples from group b .

As discussed above, it is impossible to make progress in PU settings without assumptions²². Our estimation procedure relies on three assumptions: 1) observed positives are true positives (the *positive-unlabeled* assumption common to all PU methods), 2) within each group, diagnosis s depends only on y (the *random diagnosis within group* assumption, commonly made in PU settings) and 3) the probability of having a disease conditional on symptoms remains constant across groups (the *constant $p(y|x)$* assumption, common to work in both domain adaptation^{23,24} and healthcare²⁵). Details about the required assumptions can be found in Sec. M1.1. We also provide checks to assess whether the assumptions hold (Sec. M1.5), and show that even under plausible

violations of these assumptions, PURPLE is guaranteed to produce a lower bound on the true magnitude of disparities (Sec. M1.6). An illustration of PURPLE’s behavior under violations of the PU assumption and random-diagnosis-within-group assumption is available in Sec. M1.7 and Sec. M1.8, respectively. We provide the full derivation of our estimation procedure in Sec. M1.

PURPLE recovers the true relative prevalence on synthetic data

Prior to applying PURPLE to estimate the relative prevalence of IPV, we confirm that the method can correctly recover the true prevalence on synthetic data where the true relative prevalence is known, a standard machine learning check. We compare PURPLE to four previous machine learning methods (Sec. M3) drawn from the literature on PU learning, where estimating prevalence is a critical step²⁶. We generate the synthetic data by simulating group-specific features ($p(x|g)$), and labels using a decision rule ($p(y|x)$). The two groups, a and b , correspond to 5D Gaussian distributions with different means (see Sec. M2.1 for full data generation details).

Figure 2B compares PURPLE’s performance to performance of the other methods on purely synthetic data. We evaluate each approach in both separable (in which the datapoints with $y = 1$ and the datapoints with $y = 0$ can be perfectly separated in the feature space x) and non-separable settings. We perform this comparison because existing methods rely on separability assumptions which often do not hold in realistic health settings¹⁷. PURPLE is the only method that accurately recovers the relative prevalence in both the separable and non-separable settings. We also show that PURPLE maintains consistent performance regardless of the extent to which $p(x)$, or the distribution of symptoms, differs between groups (Figure S1).

PURPLE recovers the true relative prevalence in realistic semi-synthetic health data

Having established that PURPLE outperforms previous work on synthetic data, we investigate its performance on more realistic data: specifically, MIMIC-IV¹, a dataset of electronic health records that describes $\sim 450,000$ patient hospital visits between 2008-2018. We use these records to

generate realistic semi-synthetic data to examine PURPLE’s performance on the high-dimensional, sparse data common in clinical settings. Specifically, we use the patient symptoms x — encoded as a binary one-hot vector of ICD codes — to simulate whether the patient truly has the medical condition, y . Using data in which we know y allows us to assess how accurately PURPLE recovers the relative prevalence; in contrast, if we did not simulate y , we would not have access to ground truth, and could not assess relative prevalence estimates. We simulate y for four settings: 1) a condition with common symptoms, 2) a condition that is less common among Black patients, 3) endometriosis, and 4) intimate partner violence (see Sec. M2.2 for full details).

Across the semi-synthetic settings we consider, the estimation error of previous methods is large, with some methods producing relative prevalence estimates more than 4x the true value (Fig. 2C). Further, each previous method produces both overestimates and underestimates of the true relative prevalence depending on how underreported the medical condition is. In contrast, PURPLE remains accurate across the different settings.

Quantifying the relative prevalence of intimate partner violence

We have validated PURPLE’s accuracy in recovering the relative prevalence by using synthetic and semi-synthetic datasets where the true relative prevalence is known. We now use PURPLE to estimate relative prevalence on two real datasets where the true relative prevalence is *unknown*. Specifically, we apply PURPLE to quantify the relative prevalence of the underdiagnosed condition motivating this work — intimate partner violence (IPV) — across different demographic groups.

Datasets We conduct our study using two widely-used datasets of emergency department visits: MIMIC-IV ED³ and the 2019 Nationwide Emergency Department Sample (NEDS)². MIMIC-IV describes 293,297 emergency department visits to a single, Boston-area hospital; NEDS is a nationwide sample which is approximately one hundred times as large (it contains 33.1 million emergency department visits, which, when reweighted, represent the universe of 143 million US emergency department visits in 2019). We assess results across multiple datasets to verify the

robustness of the disparities we observe. Because our sample consists of emergency department visits, we estimate the relative prevalence of IPV *conditional on going to the emergency department* — in particular, our data does not allow us to quantify disparities among populations who do not interact with the healthcare system at all²⁷. Relative prevalence estimates among patients who visit emergency departments, however, remain of interest to IPV researchers due to the unique role emergency departments play as a point of care *and* intervention on patients who suffer from IPV²⁸. For both datasets, we filter for female patients because the symptoms associated with IPV in male patients are less well understood and the constant $p(y = 1|x)$ assumption may not hold²⁹; we also filter out patients younger than 18 years old because symptoms that indicate intimate partner violence could be instances of child abuse in this patient subgroup^{30,31}. We describe all preprocessing steps in Section M2. All point estimates and uncertainties reported below represent the mean and standard deviation, respectively, across five randomized train/test splits of each dataset.

Analysis Results are plotted in Figure 3. (We also verify that PURPLE passes the assumption checks detailed in Section M1.5 in SI Figures S4, S5, S6). We find, in both datasets, that intimate partner violence is more common among patients on Medicaid compared to patients on Medicare (NEDS relative prevalence 2.44 ± 0.07 in Medicaid patients versus 0.37 ± 0.01 in Medicare patients; MIMIC-IV relative prevalence 2.65 ± 0.31 in Medicaid patients versus 0.38 ± 0.04 in Medicare patients). Of course, Medicaid is likely not the *causal* factor underlying IPV risk; rather, it acts as a proxy which identifies populations who are disproportionately affected by IPV.

Examining racial differences reveals disparities which are smaller and less consistent than disparities by insurance status. In both datasets, white patients have the lowest relative prevalence of the four race groups, and in the NEDS dataset white patients have significantly lower prevalence than non-white patients overall (relative prevalence for white patients vs. non-white patients 0.82 ± 0.02). However, in MIMIC-IV, racial disparities are more noisily estimated due to the smaller size of the dataset, yielding an ordering of race groups which is similar but not completely consistent across the two datasets. This attests to the importance of using large samples and as-

sessing results across multiple datasets.

The MIMIC-IV dataset provides information on patient marital status, allowing us to estimate that IPV is more common among patients who are “Legally Unmarried”, who are not officially married but may still be in relationships (relative prevalence 1.48 ± 0.21). The NEDS dataset provides information on the population density and estimated median household income of areas where patients live. We estimate higher rates of IPV among patients living in central metropolitan counties with population >1 million (relative prevalence 1.18 ± 0.02). We also find that IPV prevalence decreases with income (relative prevalence 1.16 ± 0.02 in the bottom income quartile versus 0.87 ± 0.03 in the top income quartile).

In Figure S3, we report the prevalence of observed IPV diagnoses — i.e., $p(s = 1|g)$ — without correcting for underdiagnosis. While often the trends are qualitatively similar, in some cases correcting for underdiagnosis is important to yield plausible trends. For example, failing to correct for underdiagnosis produces an inconsistent relationship between IPV prevalence and income which is difficult to reconcile with past work consistently documenting that IPV prevalence decreases with income^{19–21}. This suggests the importance of using methods, like PURPLE, which attempt to correct for underdiagnosis. Our income results also suggest that IPV is less likely to be correctly diagnosed in lower-income women, a finding that reflects the broader phenomenon of underdiagnosis among lower-income patients, as has been shown in the context of dementia^{32,33}, asthma^{34,35}, and depression^{36–38}.

Discussion

In this work, we provide a method for estimating relative prevalence even in the presence of underreporting, a difficult but essential task in healthcare and public health more broadly. We show that we can estimate the relative prevalence even in settings where absolute prevalence estimation is impossible, by exchanging the restrictive separability assumptions typical in the PU learning literature for the constant $p(y = 1|x)$ assumption, which is arguably more appropriate in clinical settings. Although this assumption may not hold for all settings—for example, the conditional

probability of intimate partner violence is known to be dependent on a patient’s age group³⁹—it is realistic in many settings, and we provide methods for checking its validity and a lower-bound guarantee even when it fails to hold. Based on these assumptions, we present a method for relative prevalence estimation, `PURPLE`, a complementary approach to those in the epidemiology and PU learning literature: it works when one does not have the external information which epidemiological methods generally require, and cannot make the separability assumptions PU learning methods rely on. We show `PURPLE` outperforms previous methods in terms of its ability to recover the relative prevalence on both synthetic and real health data.

We apply `PURPLE` to estimate the relative prevalence of intimate partner violence in two widely-used, large-scale datasets of emergency department visits. We find that IPV is more prevalent among patients who are on Medicaid, non-white, not legally married, in lower-income zipcodes, and in metropolitan counties. We also show that correcting for underdiagnosis produces estimates of IPV prevalence across income groups which are more plausible in light of prior work^{19–21}, highlighting the importance of modeling underdiagnosis. In general, past work on IPV disparities corroborates the plausibility of our findings. Our finding that intimate partner violence is more common among patients on Medicaid compared to patients on Medicare is consistent with earlier results that show that IPV is less common among elderly patients^{39–41}, and more common among patients who live below the poverty line^{20,42,43}. Past work documenting higher IPV prevalences among unmarried women^{44–46} and in metropolitan areas^{19,47,48} also corroborates the plausibility of our findings. Our finding that IPV is more common among non-white patients is corroborated by some past work^{7,19,49}. However, the fact that we find that racial disparities are smaller and not completely consistent across datasets is also concordant with past work documenting inconsistent racial differences across samples^{43,50–52}. This suggests the importance of using large samples, and multiple datasets, to assess how consistently and robustly racial disparities emerge. Overall, our analysis contributes to the literature on IPV disparities by using large samples; evaluating robustness across multiple datasets; and correcting for underreporting.

Our work is motivated by widespread underreporting in women’s health, and we foresee numerous opportunities for future work. PURPLE could be applied to obtain relative prevalence estimates for many other health conditions that are known to be underreported, including polycystic ovarian syndrome⁵³, endometriosis⁵⁴, and traumatic brain injuries⁵⁵. Additionally, quantifying relative prevalence in the presence of underreporting is a problem of interest in many domains beyond healthcare and public health: for example, quantifying the relative prevalence of underreported police misconduct across precincts, or quantifying the relative prevalence of underreported hate speech across demographic groups. We believe that PURPLE can also yield useful insight into disparities in these non-healthcare settings.

Data availability: Anonymized imaging and clinical data to reproduce results of this study are available online. MIMIC-IV is a publicly available database of emergency department and hospital admissions occurring between 2008 and 2019 at the Beth Israel Deaconess Medical Center. NEDS 2019 is also a publicly available Both datasets are publicly available. MIMIC-IV can be found at: <https://physionet.org/content/mimiciv/2.2/>. The HCUP NEDS 2019 database is also publicly available at: <https://www.hcup-us.ahrq.gov/nedsoverview.jsp>. Code to preprocess all datasets and reproduce all experiments can be found at <https://github.com/epierson9/invisible-conditions>.

Acknowledgments: We thank Microsoft Research seminar participants, Irene Chen, Serina Chang, Jacquelyn Campbell, Karthik Chetty, Nikhil Garg, John Gutttag, Pang Wei Koh, Allison Koenecke, Nat Roth, Priya Shanmugam, and Harini Suresh for helpful conversations. EP was supported by a Google Research Scholar award, an NSF CAREER award, a CIFAR Azrieli Global scholarship, a LinkedIn Research Award, and a Future Fund Regrant.

Competing interests: The authors declare no competing financial or non-financial interests.

Author contributions: E.P. supervised the project. E.P. and D.S. conceived of the presented method, experiments, theory, and verified the results. E.P. and D.S. wrote the manuscript. D.S. conducted the synthetic and semi-synthetic experiments, carried out the case studies for intimate

partner violence and content moderation, and created the figures. K.H. conducted analyses of the MIMIC-IV data and the NEDS data.

References

1. Johnson, A. *et al.* Mimic-iv (version 0.4). *PhysioNet* (2020).
2. Cost, H. & (HCUP), U. P. The study examined emergency department visits for diabetes using discharge data from the nationwide emergency department sample (neds).
3. Johnson, A. *et al.* Mimic-iv-ed (2021).
4. MacDorman, M. F., Declercq, E. & Thoma, M. E. Trends in maternal mortality by socio-demographic characteristics and cause of death in 27 states and the district of columbia. *Obstetrics and gynecology* **129**, 811 (2017).
5. FACT SHEET: Biden-Harris Administration Announces Initial Actions to Address the Black Maternal Health Crisis. <https://www.whitehouse.gov/briefing-room/statements-releases/2021/04/13/fact-sheet-biden-harris-administration-announces-initial-actions-to-address-the-black-maternal-health-crisis/>
Accessed: 2022-10-16.
6. Geiger, H. J. Racial and ethnic disparities in diagnosis and treatment: a review of the evidence and a consideration of causes. *Unequal treatment: Confronting racial and ethnic disparities in health care* **417** (2003).
7. Schafer, S. D., Drach, L. L., Hedberg, K. & Kohn, M. A. Using diagnostic codes to screen for intimate partner violence in oregon emergency departments and hospitals. *Public Health Reports* **123**, 628–635 (2008).
8. Lyles, R. H. *et al.* Validation data-based adjustments for outcome misclassification in logistic regression: an illustration. *Epidemiology (Cambridge, Mass.)* **22**, 589 (2011).
9. Sekar, C. C. & Deming, W. E. On a method of estimating birth and death rates and the extent of registration. *Journal of the American statistical Association* **44**, 101–115 (1949).
10. Simeone, R. S., Rhodes, W. M. & Hunt, D. E. A plan for estimating the number of “hardcore” drug users in the united states. *International journal of the addictions* **30**, 637–657 (1995).
11. Hay, G. & Smit, F. Estimating the number of drug injectors from needle exchange data. *Addiction Research & Theory* **11**, 235–243 (2003).
12. McKeganey, N., Barnard, M., Leyland, A., Coote, I. & Follet, E. Female streetworking prostitution and hiv infection in glasgow. *British Medical Journal* **305**, 801–804 (1992).

13. Hui, S. L. & Walter, S. D. Estimating the error rates of diagnostic tests. *Biometrics* 167–171 (1980).
14. Walter, S. D. & Irwig, L. M. Estimation of test error rates, disease prevalence and relative risk from misclassified data: a review. *Journal of clinical epidemiology* **41**, 923–937 (1988).
15. Pepe, M. S. & Janes, H. Insights into latent class analysis of diagnostic test performance. *Biostatistics* **8**, 474–484 (2007).
16. Lewis, F., Sanchez-Vazquez, M. & Torgerson, P. Association between covariates and disease occurrence in the presence of diagnostic error. *Epidemiology & Infection* **140**, 1515–1524 (2012).
17. Chen, J. H. & Asch, S. M. Machine learning and prediction in medicine—beyond the peak of inflated expectations. *The New England journal of medicine* **376**, 2507 (2017).
18. Davidov, D. M., Larrabee, H. & Davis, S. M. United states emergency department visits coded for intimate partner violence. *The Journal of emergency medicine* **48**, 94–100 (2015).
19. Rennison, C. & Welchans, S. Bureau of justice statistics special report: Intimate partner violence. retrieved november 12, 2007 (2000).
20. Bonomi, A. E., Trabert, B., Anderson, M. L., Kernic, M. A. & Holt, V. L. Intimate partner violence and neighborhood income: a longitudinal analysis. *Violence Against Women* **20**, 42–58 (2014).
21. Abramsky, T. *et al.* Women’s income and risk of intimate partner violence: secondary findings from the maisha cluster randomised trial in north-western tanzania. *BMC public health* **19**, 1–15 (2019).
22. Bekker, J. & Davis, J. Learning from positive and unlabeled data: A survey. *Machine Learning* **109**, 719–760 (2020).
23. Sugiyama, M., Krauledat, M. & Müller, K.-R. Covariate shift adaptation by importance weighted cross validation. *Journal of Machine Learning Research* **8** (2007).
24. Quiñonero-Candela, J., Sugiyama, M., Lawrence, N. D. & Schwaighofer, A. *Dataset shift in machine learning* (Mit Press, 2009).
25. Nestor, B. *et al.* Feature robustness in non-stationary health records: caveats to deployable model performance in common clinical machine learning tasks. In *Machine Learning for Healthcare Conference*, 381–405 (PMLR, 2019).

26. Bekker, J., Robberechts, P. & Davis, J. Beyond the selected completely at random assumption for learning from positive and unlabeled data. In *Joint European Conference on Machine Learning and Knowledge Discovery in Databases*, 71–85 (Springer, 2019).
27. Riley, W. J. Health disparities: gaps in access, quality and affordability of medical care. *Transactions of the American Clinical and Climatological Association* **123**, 167 (2012).
28. Alessandrino, F. *et al.* Intimate partner violence: a primer for radiologists to make the “invisible” visible. *Radiographics* **40**, 2080–2097 (2020).
29. Houry, D. *et al.* Differences in female and male victims and perpetrators of partner violence with respect to web scores. *Journal of interpersonal violence* **23**, 1041–1055 (2008).
30. Louwers, E. C. *et al.* Detection of child abuse in emergency departments: a multi-centre study. *Archives of disease in childhood* **96**, 422–425 (2011).
31. Loder, R. T. & Momper, L. Demographics and fracture patterns of patients presenting to us emergency departments for intimate partner violence. *JAAOS Global Research & Reviews* **4** (2020).
32. Amjad, H. *et al.* Underdiagnosis of dementia: an observational study of patterns in diagnosis and awareness in us older adults. *Journal of general internal medicine* **33**, 1131–1138 (2018).
33. Bradford, A., Kunik, M. E., Schulz, P., Williams, S. P. & Singh, H. Missed and delayed diagnosis of dementia in primary care: prevalence and contributing factors. *Alzheimer Disease & Associated Disorders* **23**, 306–314 (2009).
34. Aaron, S. D., Boulet, L. P., Reddel, H. K. & Gershon, A. S. Underdiagnosis and overdiagnosis of asthma. *American journal of respiratory and critical care medicine* **198**, 1012–1020 (2018).
35. Quinn, K., Shalowitz, M. U., Berry, C. A., Mijanovich, T. & Wolf, R. L. Racial and ethnic disparities in diagnosed and possible undiagnosed asthma among public-school children in chicago. *American journal of public health* **96**, 1599–1603 (2006).
36. Swant, E. & Wyatt, L. 200 underdiagnosis of depression among low-income, predominantly latino, type 2 diabetics. (2007).
37. Lao, C.-K., Chan, Y.-M., Tong, H. H.-Y. & Chan, A. Underdiagnosis of depression in an economically deprived population in macao, china. *Asia-Pacific Psychiatry* **8**, 70–79 (2016).
38. Sorkin, D. H. *et al.* Underdiagnosed and undertreated depression among racially/ethnically diverse patients with type 2 diabetes. *Diabetes care* **34**, 598–600 (2011).

39. Pathak, N., Dhairyawan, R. & Tariq, S. The experience of intimate partner violence among older women: A narrative review. *Maturitas* **121**, 63–75 (2019).
40. Evans, C. S., Hunold, K. M., Rosen, T. & Platts-Mills, T. F. Diagnosis of elder abuse in us emergency departments. *Journal of the American Geriatrics Society* **65**, 91–97 (2017).
41. Gerino, E., Calderera, A. M., Curti, L., Brustia, P. & Rollè, L. Intimate partner violence in the golden age: Systematic review of risk and protective factors. *Frontiers in psychology* **9**, 1595 (2018).
42. Cunradi, C. B., Caetano, R., Clark, C. & Schafer, J. Neighborhood poverty as a predictor of intimate partner violence among white, black, and hispanic couples in the united states: A multilevel analysis. *Annals of epidemiology* **10**, 297–308 (2000).
43. Mariscal, T. L., Hughes, C. M. & Modrek, S. Changes in incidents and payment methods for intimate partner violence related injuries in women residing in the united states, 2002 to 2015. *Women's health issues* **30**, 338–344 (2020).
44. Wong, J. Y.-H. *et al.* A comparison of intimate partner violence and associated physical injuries between cohabitating and married women: a 5-year medical chart review. *BMC Public Health* **16**, 1–9 (2016).
45. Abramsky, T. *et al.* What factors are associated with recent intimate partner violence? findings from the who multi-country study on women's health and domestic violence. *BMC public health* **11**, 1–17 (2011).
46. Capaldi, D. M., Knoble, N. B., Shortt, J. W. & Kim, H. K. A systematic review of risk factors for intimate partner violence. *Partner abuse* **3**, 231–280 (2012).
47. Ravi, K. E., Rai, A. & Schrag, R. V. Survivors' experiences of intimate partner violence and shelter utilization during covid-19. *Journal of family violence* **37**, 979–990 (2022).
48. DuBois, K. O., Rennison, C. M. & DeKeseredy, W. S. Intimate partner violence in small towns, dispersed rural areas, and other locations: Estimates using a reconception of settlement type. *Rural sociology* **84**, 826–852 (2019).
49. Lipsky, S., Caetano, R. & Roy-Byrne, P. Racial and ethnic disparities in police-reported intimate partner violence and risk of hospitalization among women. *Women's health issues* **19**, 109–118 (2009).
50. Cho, H. Racial differences in the prevalence of intimate partner violence against women and associated factors. *Journal of Interpersonal Violence* **27**, 344–363 (2012).

51. Domestic, E. & Violence, G.-B. 2020 report on the intersection of domestic violence, race/ethnicity and sex (2020).
52. Hart JD, B. & Klein PhD, A. J. Practical implications of current intimate partner violence research for victim advocates and service providers (2013).
53. Hillman, S. C. & Dale, J. Polycystic ovarian syndrome: an under-recognised problem? *British Journal of General Practice* **68**, 244–244 (2018).
54. Agarwal, S. K. *et al.* Clinical diagnosis of endometriosis: a call to action. *American journal of obstetrics and gynecology* **220**, 354–e1 (2019).
55. Prince, C. & Bruhns, M. E. Evaluation and treatment of mild traumatic brain injury: the role of neuropsychology. *Brain sciences* **7**, 105 (2017).
56. Elkan, C. & Noto, K. Learning classifiers from only positive and unlabeled data. In *Proceedings of the 14th ACM SIGKDD international conference on Knowledge discovery and data mining*, 213–220 (2008).
57. Bekker, J. & Davis, J. Estimating the class prior in positive and unlabeled data through decision tree induction. In *Proceedings of the AAAI Conference on Artificial Intelligence*, vol. 32 (2018).
58. Jain, S., White, M. & Radivojac, P. Estimating the class prior and posterior from noisy positives and unlabeled data. *Advances in neural information processing systems* **29** (2016).
59. Du Plessis, M. C. & Sugiyama, M. Class prior estimation from positive and unlabeled data. *IEICE TRANSACTIONS on Information and Systems* **97**, 1358–1362 (2014).
60. Northcutt, C. G., Wu, T. & Chuang, I. L. Learning with confident examples: Rank pruning for robust classification with noisy labels. *arXiv preprint arXiv:1705.01936* (2017).
61. Ramaswamy, H., Scott, C. & Tewari, A. Mixture proportion estimation via kernel embeddings of distributions. In *International conference on machine learning*, 2052–2060 (PMLR, 2016).
62. Chen, I. Y., Joshi, S., Ghassemi, M. & Ranganath, R. Probabilistic machine learning for healthcare. *Annual Review of Biomedical Data Science* **4**, 393–415 (2021).
63. Paszke, A. *et al.* Automatic differentiation in pytorch (2017).
64. Steyerberg, E. W. *et al.* Assessing the performance of prediction models: a framework for some traditional and novel measures. *Epidemiology (Cambridge, Mass.)* **21**, 128 (2010).

65. Moradi, M., Parker, M., Sneddon, A., Lopez, V. & Ellwood, D. Impact of endometriosis on women's lives: a qualitative study. *BMC women's health* **14**, 1–12 (2014).
66. Jabr, F. I. & Mani, V. An unusual cause of abdominal pain in a male patient: Endometriosis. *Avicenna Journal of Medicine* **4** (2014).
67. Wu, V., Huff, H. & Bhandari, M. Pattern of physical injury associated with intimate partner violence in women presenting to the emergency department: a systematic review and meta-analysis. *Trauma, Violence, & Abuse* **11**, 71–82 (2010).
68. Lazkecka, M., Mielniczuk, J. & Teisseyre, P. Estimating the class prior for positive and unlabelled data via logistic regression. *Advances in Data Analysis and Classification* 1–30 (2021).
69. Jaskie, K. & Spanias, A. Positive and unlabeled learning algorithms and applications: A survey. In *2019 10th International Conference on Information, Intelligence, Systems and Applications (IISA)*, 1–8 (IEEE, 2019).
70. Teisseyre, P., Mielniczuk, J. & Lazkecka, M. Different strategies of fitting logistic regression for positive and unlabelled data. In *International Conference on Computational Science*, 3–17 (Springer, 2020).
71. Furmańczyk, K., Mielniczuk, J., Rejchel, W. & Teisseyre, P. Joint estimation of posterior probability and propensity score function for positive and unlabelled data. *arXiv preprint arXiv:2209.07787* (2022).
72. Ivanov, D. Dedpul: Difference-of-estimated-densities-based positive-unlabeled learning. In *2020 19th IEEE International Conference on Machine Learning and Applications (ICMLA)*, 782–790 (IEEE, 2020).
73. Garg, S., Wu, Y., Smola, A. J., Balakrishnan, S. & Lipton, Z. Mixture proportion estimation and pu learning: A modern approach. *Advances in Neural Information Processing Systems* **34**, 8532–8544 (2021).
74. Lash, T. L. *et al.* Good practices for quantitative bias analysis. *International journal of epidemiology* **43**, 1969–1985 (2014).
75. Delgado-Rodriguez, M. & Llorca, J. Bias. *Journal of Epidemiology & Community Health* **58**, 635–641 (2004).
76. Copeland, K. T., Checkoway, H., McMichael, A. J. & Holbrook, R. H. Bias due to misclassification in the estimation of relative risk. *American journal of epidemiology* **105**, 488–495 (1977).

77. Greenland, S. & Kleinbaum, D. G. Correcting for misclassification in two-way tables and matched-pair studies. *International Journal of Epidemiology* **12**, 93–97 (1983).
78. Kristensen, P. Bias from nondifferential but dependent misclassification of exposure and outcome. *Epidemiology* 210–215 (1992).
79. Neuhaus, J. M. Bias and efficiency loss due to misclassified responses in binary regression. *Biometrika* **86**, 843–855 (1999).
80. Reiczigel, J., Singer, J. & Lang, Z. Exact inference for the risk ratio with an imperfect diagnostic test. *Epidemiology & Infection* **145**, 187–193 (2017).
81. Magder, L. S. & Hughes, J. P. Logistic regression when the outcome is measured with uncertainty. *American journal of epidemiology* **146**, 195–203 (1997).
82. Diggle, P. J. Estimating prevalence using an imperfect test. *Epidemiology Research International* **2011** (2011).
83. Lewis, F. I. & Torgerson, P. R. A tutorial in estimating the prevalence of disease in humans and animals in the absence of a gold standard diagnostic. *Emerging themes in epidemiology* **9**, 1–8 (2012).
84. Haine, D., Dohoo, I. & Dufour, S. Selection and misclassification biases in longitudinal studies. *Frontiers in veterinary science* **5**, 99 (2018).
85. Scott, C. A rate of convergence for mixture proportion estimation, with application to learning from noisy labels. In *Artificial Intelligence and Statistics*, 838–846 (PMLR, 2015).
86. Scott, D. & Sain, S. Multi-dimensional density estimation handbook of statistics vol 23 data mining and computational statistics ed cr rao and ej wegman (2004).
87. Christoffel, M., Niu, G. & Sugiyama, M. Class-prior estimation for learning from positive and unlabeled data. In *Asian Conference on Machine Learning*, 221–236 (PMLR, 2016).
88. Liu, T. & Tao, D. Classification with noisy labels by importance reweighting. *IEEE Transactions on pattern analysis and machine intelligence* **38**, 447–461 (2015).
89. Blanchard, G., Lee, G. & Scott, C. Semi-supervised novelty detection. *The Journal of Machine Learning Research* **11**, 2973–3009 (2010).
90. Leone, M. *et al.* Social network analysis to characterize women victims of violence. *BMC public health* **19**, 1–11 (2019).

91. Halpern, L. R., Perciaccante, V. J., Hayes, C., Susarla, S. & Dodson, T. B. A protocol to diagnose intimate partner violence in the emergency department. *Journal of Trauma and Acute Care Surgery* **60**, 1101–1105 (2006).

1 Methods

2 M1 PURPLE: Positive Unlabeled Prevalence Estimator

3 PURPLE estimates $p(y = 1|x)$ up to a constant multiplicative factor in order to estimate the relative
4 prevalence of a condition y . Underlying this procedure are two insights: first, that estimating
5 $p(y = 1|x)$ up to a constant factor suffices to estimate the relative prevalence, and second, that it
6 is possible to produce this estimate using the observed labels s , symptoms x , and group statuses
7 g . We first describe the three assumptions underlying PURPLE, and show how these statements
8 follow from them in Sections M1.2 and M1.3. We describe implementation details in Sec. M1.4.
9 We provide checks to determine whether PURPLE’s assumptions hold true (Sec. M1.5) and show
10 that even under a plausible violation of our assumptions, PURPLE produces a lower bound on the
11 true magnitude of disparities (Sec. M1.6).

12 M1.1 Assumptions

13 Neither the exact prevalence nor the relative prevalence can be recovered without making assump-
14 tions about the data generating process: intuitively, without further assumptions, it is impossible
15 to distinguish between whether a medical condition is truly rare or merely rarely *diagnosed*. We
16 adopt terminology standard in the PU learning literature and assume that we have access to three
17 pieces of data for the i th example: a feature vector x_i ; a group variable g_i ; and a binary observed
18 label s_i . We let y_i denote the true (unobserved) label. In healthcare, example i may correspond to a
19 specific patient and their presenting symptoms (x_i), race (g_i), and observed diagnosis (s_i). Here, y_i
20 corresponds to whether the patient truly *has* the medical condition. This is an unobserved binary
21 variable and because the medical condition is underreported, not all patients who truly have the
22 condition are diagnosed with it, so $p(s_i = 1|y_i = 1) < 1$. Because we are interested in health dis-
23 parities, we focus on groups g defined by sensitive attributes (e.g., gender, race, or socioeconomic
24 status) but our method is applicable to any set of groups for which our assumptions hold. We make
25 three assumptions:

- 26 1. *No False Positives*: We assume that examples labeled as positive ($s = 1$) are truly positive

27 $(y = 1)$: i.e., $p(y = 0|s = 1) = 0$ (and thus, by Bayes’ rule, $p(s = 1|y = 0) = 0$). This is the
28 positive unlabeled assumption and is the foundational assumption of PU learning methods⁵⁶.

29 2. *Random Diagnosis within Groups*: We assume that positive examples within a specific group
30 are equally likely to be labeled as positive: $p(s = 1|y = 1, g = a) = c_a$, where c_a repre-
31 sents the diagnosis frequency of group a (i.e. the probability that a positive case is diag-
32 nosed as such). Borrowing terminology from PU learning, this amounts to the commonly
33 made Selected-Completely-at-Random assumption⁵⁷ within each group. We allow c_a to vary
34 across groups to allow for group-specific underdiagnosis rates.

35 3. *Constant $p(y = 1|x)$ between Groups*: We assume that $p(y = 1|x)$ remains constant across
36 groups: examples in different groups with the same features are equally likely to be true
37 positives. In the medical setting, this means that patients in different groups with the same
38 symptoms have the same probability of truly having a condition. This is equivalent to as-
39 suming only *covariate shift* between groups, a commonly made assumption in the literature
40 on domain adaptation^{23,24} and healthcare²⁵.

41 Notably, we make no assumptions about the separability of the positive and negative distributions.
42 Past work in PU learning has shown that the true prevalence $p(y = 1)$ can be recovered under a
43 restrictive set of assumptions about the structure of the positive and negative distributions⁵⁸, which
44 we refer to as “separability assumptions”. Many PU learning methods assume that the positive
45 distribution is not completely contained within the negative distribution: in healthcare, this means
46 there is a region of the feature space where all examples are true positives^{56,59–61} (Fig. 2A). This
47 assumption is unrealistic in medical settings because it is unlikely that a set of symptoms maps to
48 a diagnosis with 100% probability⁶², and as a result, PURPLE makes no such assumption.

49 While it is necessary to make assumptions to infer the relative prevalence, no assumptions will hold
50 on all datasets, a point we consider in the Discussion. To ensure PURPLE is applied to appropriate
51 datasets, we provide two checks for violations of PURPLE’s assumptions (Sec. M1.5). We also

52 show that even under a plausible violation of the *Constant* $p(y = 1|x)$ assumption, PURPLE
 53 provides a useful *lower bound* on the magnitude of health disparities (Sec. M1.6).

54 M1.2 Deriving the Relative Prevalence

55 Here we show that a constant factor multiplicative approximation of $p(y = 1|x)$ recovers the
 56 relative prevalence between groups a and b ($\rho_{a,b}$) exactly. The derivation is as follows:

$$\rho_{a,b} := \frac{p(y = 1|g = a)}{p(y = 1|g = b)} \quad (3)$$

$$= \frac{\sum_x p(y = 1|x, g = a)p(x|g = a)}{\sum_x p(y = 1|x, g = b)p(x|g = b)} \quad (4)$$

$$= \frac{\sum_x p(y = 1|x)p(x|g = a)}{\sum_x p(y = 1|x)p(x|g = b)} \quad (5)$$

$$= \frac{\sum_x \hat{p}(y = 1|x)p(x|g = a)}{\sum_x \hat{p}(y = 1|x)p(x|g = b)} \quad (6)$$

for all $\hat{p}(y = 1|x) \propto p(y = 1|x)$

57 where Eqn. 5 follows from the constant $p(y = 1|x)$ assumption and Eqn. 6 follows because
 58 estimates of $p(y = 1|x)$ up to a constant multiplicative factor will yield a constant term in the
 59 numerator and denominator which cancels. Thus, estimates of $p(y = 1|x)$ up to a constant mul-
 60 tiplicative factor suffice to compute the relative prevalence. $p(x|g)$ is directly observable from the
 61 data, so we can estimate the numerator as the mean of $\hat{p}(y = 1|x)$ over all x in group a , and
 62 similarly estimate the denominator as the mean of $\hat{p}(y = 1|x)$ over all x in group b .

63 M1.3 Estimating $p(y = 1|x)$ up to a constant multiplicative factor

64 We have shown that, if we can estimate $p(y = 1|x)$ up to a constant multiplicative factor, we can
 65 use this estimate to compute the relative prevalence $\rho_{a,b}$. Now we show how to estimate $p(y = 1|x)$
 66 up to a constant multiplicative factor. We do so by applying our three assumptions to derive an
 67 decomposition for $p(s = 1|x, g)$:

$$p(s = 1|x, g) = p(y = 1|x, g)p(s = 1|y = 1, x, g) \quad (7)$$

$$+ p(y = 0|x, g)p(s = 1|y = 0, x, g)$$

$$= p(y = 1|x, g)p(s = 1|y = 1, x, g) \quad (8)$$

$$= p(y = 1|x, g)p(s = 1|y = 1, g) \quad (9)$$

$$= p(y = 1|x)p(s = 1|y = 1, g) \quad (10)$$

68 Applying the *No False Positives* assumption allows us to remove the second term in Eqn. 7,
 69 producing Eqn. 8. The *Random Diagnosis within Groups* assumption removes the dependence of
 70 the diagnosis probability on x , leading to Eqn. 9. The *Constant* $p(y = 1|x)$ assumption leads to
 71 Eqn. 10.

72 Thus, $p(s = 1|x, g)$ can be decomposed as the product of two terms: the probability the patient
 73 truly has the condition given their symptoms, $p(y = 1|x)$, and the probability that true positives
 74 are correctly diagnosed, $p(s = 1|y = 1, g)$. The fact that the second term varies across groups
 75 accounts for group-specific underdiagnosis. This decomposition can be fit via maximum likelihood
 76 estimation with respect to the empirical $p(s = 1|x, g)$, since s , x , and g are observed. Note that this
 77 only allows estimation of the two terms on the right side of Eqn. 10 up to constant multiplicative
 78 factors, since we can multiply $p(y = 1|x)$ by a non-negative β and divide $p(s = 1|y = 1, g)$ by
 79 β while leaving our estimate of $p(s = 1|x, g)$ unchanged. However, constant-factor estimation
 80 of $p(y = 1|x)$ suffices to estimate the relative prevalence. Concretely, we estimate $p(y = 1|x)$
 81 and $p(s = 1|y = 1, g)$ up to constant multiplicative factors by fitting to $p(s = 1|x, g)$; we then
 82 use our constant-factor estimate of $p(y = 1|x)$ to estimate the relative prevalence as described in
 83 §M1.2.

84 We note that the probabilistic model described by Eqn. 10 has been previously applied to estimate
 85 absolute prevalence in PU settings²⁶. Our novel contribution is to derive a precise set of assump-
 86 tions in which this probabilistic model can be used to estimate *relative* prevalence, and provide an
 87 estimation method to do so.

88 M1.4 Implementation

89 Thus far, we have shown that it is possible to estimate the relative prevalence of an underreported
90 condition by estimating $p(y = 1|x)$ up to a constant factor and provided a way to conduct this esti-
91 mation given only the observed data. One can apply PURPLE to a new dataset in two steps:

- 92 1. Estimate $p(y = 1|x)$ up to a constant multiplicative factor using the observed diagnoses, and
93 the following probabilistic model:

$$\hat{p}(s = 1|g, x) = \hat{p}(y = 1|x)\hat{p}(s = 1|y = 1, g) \quad (11)$$

- 94 2. Plug our constant multiplicative factor estimate, $\hat{p}(y = 1|x)$, into Eqn. 6 to produce the
95 relative prevalence estimate. Specifically, we estimate the relative prevalence $\rho_{a,b}$ as:

$$\frac{\sum_x \hat{p}(y = 1|x)\hat{p}(x|g = a)}{\sum_x \hat{p}(y = 1|x)\hat{p}(x|g = b)} \quad (12)$$

96 In practice, we can compute this fraction simply by taking the mean value of $\hat{p}(y = 1|x)$ in
97 each group to compute the numerator and denominator.

98 We implement the model in PyTorch⁶³ using a single-layer neural network to represent $\hat{p}(y = 1|x)$
99 and group-specific parameters $c_g = \hat{p}(s = 1|y = 1, g)$ for each group g . Note that a single layer
100 neural network, followed by a logistic activation, is functionally equivalent to a logistic regression,
101 as they both learn a linear transformation of the input features followed by a logistic transforma-
102 tion to produce a predicted probability of the positive class. We train the model using the Adam
103 optimizer with default parameters (i.e. a learning rate of .001, epsilon of 10^{-8} , and weight de-
104 cay of 0) and implement early stopping based on the cross-entropy loss on the held-out validation
105 set. For the semi-synthetic and real data, we use L1 regularization because these experiments are
106 conducted on high-dimensional vectors, most of which we expect to be unrelated to the medical
107 condition, and select the regularization parameter $\lambda \in [10^{-2}, 10^{-3}, 10^{-4}, 10^{-5}, 10^{-6}, 0]$ using the
108 held-out validation set by maximizing the AUC with respect to the diagnosis labels s . While we
109 use a single-layer neural network because our symptoms x are one-hot encoded and we do not an-

110 anticipate interactions between symptoms, our approach is general and could be applied with deeper
111 neural network architectures to accommodate interactions and nonlinearities.

112 **M1.5 Assumption Checks**

113 Like all PU learning methods, PURPLE must rely on assumptions. To prevent users from applying
114 PURPLE to datasets where these assumptions do not hold, we provide two empirical tests whose
115 failure implies at least one of the underlying assumptions fails:

- 116 • *Compare model fit of PURPLE to unconstrained model.* If PURPLE’s assumptions hold,
117 the diagnosis likelihood $p(s = 1|x, g)$ decomposes as the product of two terms: $p(s =$
118 $1|x, g) = p(y = 1|x)p(s = 1|y = 1, g)$. This is a constrained model of $p(s = 1|x, g)$:
119 for example, it does not allow for interaction terms between group g and symptoms x . We
120 can compare the performance of PURPLE to a fully unconstrained model for $p(s = 1|x, g)$
121 which allows, for example, these interaction terms. If the unconstrained model better fits the
122 data, metrics including the AUC and AUPRC will be higher on a held-out set of patients. If
123 the constrained and unconstrained models exhibit similar performance, it is still possible for
124 one of the assumptions to not be true; however, if the models exhibit different performance,
125 it is a sign that PURPLE’s assumptions are not appropriate.
- 126 • *Compare calibration across groups.* PURPLE estimates a probabilistic model of diagnosis,
127 $p(s = 1|x, g)$, which means we can check how well the outputted probabilities reflect the real
128 data by examining model calibration, a standard check⁶⁴. Concretely, we expect that a pro-
129 portion z of examples that our model gives a probability z of receiving a positive diagnosis
130 truly receive a positive diagnosis, and we expect this to be true for each group. Violations of
131 PURPLE’s assumptions will often cause group-specific calibration to not hold. For example,
132 if $p(y = 1|x)$ differs between groups beyond a scalar constant factor, PURPLE’s estimate of
133 $p(s = 1|x, g)$ cannot be correct for both groups (since PURPLE assumes $p(y = 1|x)$ remains
134 constant).

135 We note that these assumption checks cannot rule out all forms of model misspecification—and,
136 indeed, no assumption checks can. Since only x , g , and s are observed, it is impossible to prove
137 anything about the distribution of y . However, the assumption checks will rule out some forms
138 of model misspecification, and guide users away from datasets where applying PURPLE is clearly
139 inappropriate.

140 **M1.6 Robustness to Violations of the Constant $p(y|x)$ Assumption**

141 In this section we show that under a plausible violation of the central new assumption of our work
142 (constant $p(y = 1|x)$ between groups), PURPLE produces a *lower bound* on the magnitude of
143 disparities. This lower bound is useful because we can be confident that if PURPLE infers that a
144 group suffers disproportionately from a condition, that is in fact the case, and we can be confident
145 in targeting policy to that group.

146 Specifically, we relax the assumption of constant $p(y = 1|x)$ across groups by assuming that if
147 group A has a higher overall prevalence of a condition than group B — i.e., $p(y = 1|g = A) >$
148 $p(y = 1|g = B)$ — group A also has a higher prevalence by a constant factor given the same set
149 of symptoms — i.e., $p(y = 1|x, g = A) = \alpha \cdot p(y = 1|x, g = B)$, $\alpha > 1$. This assumption is a
150 reasonable one: when a condition is more prevalent in one group than another, the same symptoms
151 plausibly correspond to higher posterior probabilities $p(y = 1|x)$ in the disproportionately affected
152 group. For example, female patients are more likely than male patients to be victims of intimate
153 partner violence overall²⁹, and if a woman and a man arrive in a hospital with the same injuries,
154 doctors are plausibly more likely to suspect intimate partner violence as the cause of the woman’s
155 injuries.

156 **Proof.** Without loss of generality, assume that group A is the group with higher overall disease
157 prevalence: $p(y = 1|g = A) > p(y = 1|g = B)$. We make the following assumptions:

- 158 1. Disease prevalence in group A conditional on symptoms is higher by a constant multiplica-
159 tive factor: $p(y = 1|x, g = A) = \alpha \cdot p(y = 1|x, g = B)$, $\alpha > 1$.

160 2. The other PURPLE assumptions hold: that is, $p(y = 1|s = 1) = 1$ (PU assumption) and
 161 $p(s = 1|y = 1, g, x) = p(s = 1|y = 1, g)$ (random diagnosis within groups).

162 Under these assumptions, we show that PURPLE's estimate provides a lower bound on the true
 163 relative prevalence. As before, we use p to denote the true probabilities in the underlying data
 164 distribution and \hat{p} to denote PURPLE's estimates of these probabilities. We have

$$\begin{aligned} p(s = 1|x, g = A) &= p(s = 1|y = 1, g = A) \cdot p(y = 1|x, g = B) \cdot \alpha \\ p(s = 1|x, g = B) &= p(s = 1|y = 1, g = B) \cdot p(y = 1|x, g = B) \end{aligned}$$

165 PURPLE estimates $\hat{p}(s = 1|x, g) = \hat{p}(s = 1|y = 1, g) \cdot \hat{p}(y = 1|x)$. It can minimize the cross-
 166 entropy loss by achieving an estimate $\hat{p}(s = 1|x, g)$ which matches the true $p(s = 1|x, g)$ by
 167 setting:

$$\begin{aligned} \hat{p}(y = 1|x) &= \beta \cdot p(y = 1|x, g = B) \\ \hat{p}(s = 1|y = 1, g = A) &= \frac{1}{\beta} \cdot \alpha \cdot p(s = 1|y = 1, g = A) \\ \hat{p}(s = 1|y = 1, g = B) &= \frac{1}{\beta} \cdot p(s = 1|y = 1, g = B) \end{aligned}$$

168 where β is a positive constant (this captures the fact that, as discussed previously, PURPLE only
 169 ever estimates $p(y = 1|x)$ up to a constant multiplicative factor). In other words, PURPLE can
 170 perfectly match the true probabilities $p(s = 1|g, x)$ by pushing the variation across groups in
 171 $p(y = 1|x)$ into $\hat{p}(s = 1|y = 1, g)$ (since PURPLE assumes $\hat{p}(y = 1|x)$ remains constant across
 172 groups.) Given its estimate $\hat{p}(y = 1|x)$, PURPLE's estimate $\hat{\rho}_{A,B}$ of the relative prevalence is

$$\begin{aligned} \hat{\rho}_{A,B} &= \frac{\sum_{x \in \mathcal{A}} \hat{p}(y = 1|x)}{\sum_{x \in \mathcal{B}} \hat{p}(y = 1|x)} \\ &= \frac{\sum_{x \in \mathcal{A}} \beta \cdot p(y = 1|x, g = B)}{\sum_{x \in \mathcal{B}} \beta \cdot p(y = 1|x, g = B)} \\ &< \frac{\sum_{x \in \mathcal{A}} p(y = 1|x, g = A)}{\sum_{x \in \mathcal{B}} p(y = 1|x, g = B)} \\ &= \rho_{A,B} \end{aligned}$$

173 so PURPLE's estimate $\hat{\rho}_{A,B}$ provides a lower bound on the true relative prevalence $\rho_{A,B}$.

174 **Empirical Validation** We verify this behavior empirically under synthetic violations of the con-
175 stant $p(y|x)$ assumption, again using the synthetic data described in §M2.1. Concretely, we vary
176 the difference in the probability of a positive case between group a and group b ($p(y = 1|x, g =$
177 $a) - p(y = 1|x, g = b)$), where $p(y = 1|g = a) \geq p(y = 1|g = b)$.

178 Fig. S1B demonstrates how PURPLE consistently underestimates the true relative prevalence be-
179 havior empirically by plotting PURPLE’s behavior over a range of values for α , where $\alpha \in [0, 1]$
180 and $\alpha p(y = 1|x, g = a) = p(y = 1|x, g = b)$. In each case, PURPLE provides a lower bound on
181 the true relative prevalence. We replicate this analysis for varying separations of the group-specific
182 Gaussian distributions, where darker shades of purple correspond to group-specific distributions
183 that are further from one another.

184 M1.7 Effect of Positive-Unlabeled Assumption Violations

185 Here we demonstrate how PURPLE’s performance varies over when the positive-unlabeled as-
186 sumption is violated, meaning that the sample of observed positives contains some number of
187 negatives. This can arise if the diagnostic used to create the set of observed positives exhibits
188 a non-zero false positive rate. In Figure S2A, we plot the behavior of PURPLE as we increase
189 the extent to which the setting violates the PU assumption; specifically, we vary the percentage
190 of the observed positives that truly are negative — $p(y = 0|s = 1)$ — from 0% to 20%. When
191 $p(y = 0|s = 1) = 0$, this is equivalent to the positive-unlabeled assumption and PURPLE recovers
192 the relative prevalence exactly, as expected. At greater violations of the PU assumption, PURPLE’s
193 performance degrades somewhat, as expected.

194 M1.8 Effect of Random-Diagnosis-Within-Groups Assumption Violations

195 We illustrate PURPLE’s behavior under violations of the random-diagnosis-within-groups assump-
196 tion in Figure S2B. The assumption states that the probability that a true positive is diagnosed as
197 such does not depend on x , or that $p(s = 1|y = 1, g, x) = p(s = 1|y = 1, g)$. We simulate
198 violations of the assumption by generating s according to $p(s = 1|y = 1, g, x) = c_g \cdot \sigma(\beta \cdot x_0)$.
199 In other words, the diagnosis frequency for group g is scaled by the sigmoid function of parameter

200 β multiplied by the first component of x . For $\beta = 0$, the setting adheres to the random-diagnosis-
 201 within-groups assumption. Higher values of β translate to a higher correlation between the diag-
 202 nosis probability and x_0 . As Figure S2B demonstrates, PURPLE recovers the relative prevalence
 203 under no violation of the assumption ($\beta = 0$), and incurs small errors in the estimated relative
 204 prevalence as β increases, as expected.

205 M2 Datasets

206 We make use of five datasets. We begin with two synthetic datasets: *Gauss-Synth*, a completely
 207 synthetic dataset, and *MIMIC-Semi-Synth*, a semi-synthetic dataset based on real health data. We
 208 then apply PURPLE to three non-synthetic datasets: *MIMIC-IV ED*, a dataset of electronic health
 209 records collected from a single hospital in the Boston area, and *NEDS*, a dataset of emergency
 210 department visits occurring in the US in 2019.

211 We begin with synthetic and semi-synthetic data so that the ground truth labels y are known, as is
 212 standard in the PU learning literature²², enabling us to assess how well methods recover the relative
 213 prevalence. To assess performance of all methods in our synthetic and semi-synthetic experiments,
 214 we report the mean ratio of the estimated relative prevalence to the true relative prevalence over 5
 215 random train/test splits of the dataset; values closer to 1 correspond to better performance. Code to
 216 reproduce all experiments can be found at <https://github.com/epierson9/invisible-conditions>.

217 M2.1 Gauss-Synth

218 We generate completely synthetic data by simulating group-specific features ($p(x|g)$), and labels
 219 using a decision rule ($p(y|x)$). Formally, we simulate groups a and b using two 5D Gaussian
 220 distributions with different means:

$$x_i \sim \begin{cases} \mathcal{N}_5(-\mathbf{1}, 16 \cdot \mathbf{1}) & \text{if } g_i = a \\ \mathcal{N}_5(\mathbf{1}, 16 \cdot \mathbf{1}) & \text{if } g_i = b \end{cases} \quad (13)$$

221 The likelihood function ($p(y = 1|x)$) is a logistic function of the signed distance to a hyperplane
 222 through the origin. Observed labels s are drawn such that positive labels in group i are observed
 223 with a probability of c_{g_i} . The generative model for y and s is:

$$y_i \sim \text{Bernoulli}(\sigma(\mathbf{1}^T x_i / \|\mathbf{1}\|)) \quad (14)$$

$$s_i \sim \text{Bernoulli}(c_{g_i} y_i) \quad (15)$$

224 where σ represents a logistic function ($\sigma(x) = \frac{1}{1+e^{-x}}$) and c_{g_i} is the group-specific diagnosis
 225 frequency for g_i . We draw 10,000 observations for group a and 20,000 for group b . We create
 226 the separable data by modifying the generative model described above, which does not generate
 227 separable data. Specifically, we replace each $p(y = 1|x) > 0.5$ with $p(y = 1|x) = 1$ and each
 228 $p(y = 1|x) < 0.5$ with $p(y = 1|x) = 0$, and remove the 40% of the data closest to the original
 229 decision boundary to ensure the classes are cleanly separable, as illustrated in Figure 2A.

230 M2.2 MIMIC-Semi-Synth

231 We generate semi-synthetic data using MIMIC-IV, a public dataset of real patient visits to a Boston-
 232 area hospital over the course of 2008-2018.¹ We filter out ICD codes that appear 10 or fewer times,
 233 leaving 5,544 unique ICD codes. Each feature vector x_i is a one-hot vector corresponding to the
 234 ICD codes assigned in a particular patient visit to the hospital. We generate true labels y based
 235 on a set of suspicious symptoms. Formally, this replaces Equation (15) in our generative model
 236 with:

$$y_i \sim \text{Bernoulli}(\sigma(v_{sym}^T \mathbf{x}_i / \|v_{sym}\|)) \quad (16)$$

237 where v_{sym} is a one-hot encoding of the suspicious symptoms and $v_{sym}^T x_i$ corresponds to the num-
 238 ber of suspicious symptoms present during a hospital visit. Thus, the probability a patient has a

239 medical condition is a logistic function of the number of suspicious symptoms. As before, we have
240 $s_i \sim \text{Bernoulli}(c_{g_i} y_i)$.

241 In all experiments, we compute the relative prevalence for Black (group a) versus white (group b)
242 patients since these are the largest race groups in MIMIC data. We filter the dataset for patients
243 belonging to each group. However, our method can be applied to more than 2 groups, as described
244 above. To assess how our method performs under diverse conditions, we experiment with selecting
245 the suspicious symptoms v_{sym} in four different ways:

246 **Common Symptoms** We identify the 50 most common ICD codes in MIMIC-IV and randomly
247 select 25 to be suspicious symptoms (Table S1). Group a consists of 73,090 visits from Black
248 patients ($p(y = 1|g = a) = 0.157$) and group b consists of 305,002 visits from White patients
249 ($p(y = 1|g = b) = 0.185$).

250 **High Relative Prevalence Symptoms** We filter out ICD codes that appear fewer than 50 times
251 in each group and patients less than 18 years old. After ranking the ICD codes by relative
252 prevalence—prevalence among visits by white patients, divided by prevalence among visits by
253 Black patients—we select the top 10 ICD codes as our suspicious symptom set (Table S2). Group
254 a contains 14,618 visits from Black patients $p(y = 1|g = a) = 0.061$ and group b contains 61,000
255 visits from white patients ($p(y = 1|g = b) = 0.098$).

256 **Correlated Symptoms** We consider endometriosis, a widely under-diagnosed condition⁶⁵. We
257 define our suspicious symptoms as the symptoms most highly associated with known endometriosis
258 codes. We first identify a set of patients who receive any one of 10 gold-standard ICD en-
259 dometriosis diagnosis codes (Table S3). We then identify the ICD codes which are most highly
260 associated with a gold-standard diagnosis of endometriosis: for each ICD code, we compute the ra-
261 tio $\frac{\text{prevalence of ICD code among endometriosis patients}}{\text{prevalence of ICD code among all patients}}$. We define our suspicious symptoms as the 25 ICD codes
262 with the highest value of this ratio, which includes known endometriosis symptoms such as “Ex-
263 cessive and frequent menstruation with regular cycle” and “Pelvic and perineal pain” (Table S4).

264 We do not include the 10 ICD codes used to determine the 25 suspicious symptoms in x . We filter
265 for female patients because endometriosis is extremely rare among male patients⁶⁶, leaving 47,138
266 unique hospital visits from Black patients ($p(y = 1|g = a) = 0.0534$) and 165,653 unique hospital
267 visits from white patients ($p(y = 1|g = a) = 0.0495$).

268 **Recognized Symptoms for IPV** Prior work has found that suspicious symptoms for IPV include
269 head, neck and facial injuries⁶⁷. The symptoms in this experiment consist of the 100 ICD codes
270 corresponding to these injuries (Table S5). We filter for female patients because the symptoms
271 associated with IPV in male patients are not well understood²⁹. We also filter out patients less than
272 18 years old because it is difficult to distinguish between intimate partner violence and child abuse
273 in minors. This results in a dataset with $p(y = 1|g = a) = 0.0541$ (25,546 unique patient visits)
274 and $p(y = 1|g = b) = 0.0568$ (80,227 unique patient visits).

275 In Sections M2.3 and M2.4 we describe construction of the two non-synthetic datasets, MIMIC-IV
276 and NEDS. In all these datasets, y is unknown, so we need only define the features x and known
277 positive examples in which $s = 1$.

278 M2.3 MIMIC-IV ED

279 **Data Filtering** MIMIC-IV contains two related databases: one representing diagnoses made
280 in the hospital (which we will refer to as the hospital database) and one representing diagnoses
281 made in the emergency department. There are slight inconsistencies between the two, as is to be
282 expected; for example, one emergency department stay can be associated with multiple unique hos-
283 pital admissions. We exclude 600 hospital admissions linked to multiple emergency department
284 stays, and exclude 59 emergency department stays associated with invalid hospital admissions.
285 For emergency department stays that result in a hospital admission, we include all diagnoses as-
286 signed in the emergency department or hospital. We also include patient visits that appear only in
287 the hospital database, but indicate admission through the emergency department via the “admis-
288 sion_location” field. We provide code to replicate these preprocessing steps.

289 We further filter for patients who are female and above 18. We do so because we are interested
290 in the relative prevalence of intimate partner violence between subgroups of adult female patients.
291 This leaves 293,297 individual hospital visits over 133,470 unique patients. For each demographic
292 attribute we wish to analyze disparities over (ethnicity, insurance status, and marital status), we also
293 filter out patients who are missing data for this attribute. This translates to 192,768 stays across
294 marital statuses, 208,512 stays across ethnicities, and 108,948 stays across insurance statuses. We
295 have significantly fewer stays in the insurance subgroups because we only patients for whom the
296 insurance status is known (i.e. Medicare and Medicaid recipients). We produce 5 randomized
297 dataset splits, where we reserve 60% of the data for training, 20% for validation, and 20% for
298 testing. Each patient appears in only one of these sets.

299 **Defining features x** We represent each patient visit as a one-hot encoding of the ICD codes
300 assigned. Concretely, 15,699 features represent each patient visit, where each feature corresponds
301 to the presence or absence of one ICD code (across the ICD-9 and ICD-10 standards). Note that
302 this is different from the semi-synthetic set-up and we do *not* filter out codes that appeared fewer
303 than 10 times. We do this because IPV itself is rare, and we do not want to exclude symptoms
304 which are predictive of IPV and do not occur frequently.

305 **Defining $s = 1$** To define examples where $s = 1$ (known positive examples) we use criteria for
306 reported instances of intimate partner violence from prior work. The most specific code is E967.3,
307 or "Battering by an intimate partner", drawn from the ICD-9 standard. Other codes include V6111,
308 or "Counseling for victim of spousal or partner abuse". The full code set can be found in Table
309 S6. If a patient receives any one of the the codes in the positive code set, the visit is deemed to be
310 positively labeled for intimate partner violence.

311 **Defining g** We define the groups over which we quantify disparities via demographic variables
312 associated with each electronic health record. These include race/ethnicity (Black, white, Asian,
313 Hispanic/Latino), insurance status (Medicare or Medicaid), and marital status (Legally Unmarried,
314 Married, Divorced).

315 M2.4 NEDS

316 The National Emergency Department Sample (NEDS) is the largest publicly available, all-payer
317 database describing visits to hospital-owned emergency departments in the US, and is commonly
318 used in studies of disease prevalence. In this work, we make use of NEDS 2019. The survey from
319 this year produced a dataset containing 33.1 million visits, which represent the 143 million total
320 visits occurring in hospital-owned EDs across the US in 2019. To create nationally representative
321 estimates, NEDS releases “discharge weights”, which allow the analyst to reweight estimates to
322 represent the universe of emergency department visits. We follow this procedure to reweight our
323 relative prevalence estimates.

324 **Data Filtering** As with MIMIC-IV, we include visits from patients who are female and above
325 the age of 18. The resulting dataset contains 15,357,528 visits.

326 **Defining features x** As before, we treat the ICD codes logged during a visit as the input features,
327 as a proxy for the symptoms a patient presents with. The feature set consists of 19,710 ICD-10
328 codes (excluding those used to identify positive cases, as described in the next section), which we
329 one-hot encode to create features for each ED visit.

330 **Defining $s = 1$** We use the same criteria to identify positive cases as with MIMIC-IV: we con-
331 sider a case to be labeled positive if it is associated with if it has any of the codes in Table S6.

332 **Defining g** We define groups according to race/ethnicity groups, insurance status, income quar-
333 tile, and urban/rural designation. Income quartile is calculated using the estimated median house-
334 hold income in the patient’s zipcode. In 2019, the first quartile corresponds to an estimated median
335 household income between \$0 and \$48k, the second to \$48k to \$61k, the third to \$61k - \$82k, and
336 the fourth to the remaining zipcodes. The urban/rural designations are based on the population of
337 the patient’s home county. From most to least rural, the four categories are: 50k residents to 250k
338 residents, 250k residents to 1 million residents, 1 million residents in a fringe metropolitan county,
339 and 1 million residents in a central metropolitan county.

340 M3 Baselines

341 Each of the baseline methods described below is designed to estimate the *absolute* prevalence.
342 To obtain the relative prevalence, we apply each baseline to groups a and b individually to ob-
343 tain estimates of the absolute prevalence in each group; we then divide the resulting quantities to
344 produce an estimate of the relative prevalence. To provide consistent comparisons, we constrain
345 each baseline to the use same function class as PURPLE. We do not compare to baselines in the
346 epidemiology literature because they assume access to external information (e.g. diagnostic accu-
347 racy) that is often not available; we also do not consider work that places parametric assumptions
348 on $p(y = 1|x)$ ⁶⁸⁻⁷¹ because these assumptions will not hold in general.

- 349 • *Negative*: Assigns all unlabeled examples a negative label. This approach replaces $p(y =$
350 $1|x)$ with $p(s = 1|x)$ and assumes no underreporting occurs. Past work refers to this model
351 as a *nontraditional classifier*⁵⁶ (NTC). We use *sklearn*'s logistic regression implementation
352 with no regularization and default settings for all other hyperparameters, trained with target
353 s .
- 354 • *KM2*: Models the distribution of unlabeled examples as a mixture of the positive and neg-
355 ative distribution and estimates the proportion of positives using a kernel mean embedding
356 approach⁶¹. This method is known to perform poorly on large datasets with many features⁷².
357 KM2 assumes that there exists a function that only selects positive examples.
- 358 • *DEDPUL*: Uses an NTC to map each example to a predicted probability of being labeled,
359 and performs mixture proportion estimation using the classifier's outputs on the unlabeled
360 sample⁷². Specifically, the method applies heuristics to the estimated densities of the positive
361 and unlabeled distribution.
- 362 • *BBE*: Identifies a small subset of positive examples using the outputs of an NTC on the
363 positive and unlabeled sample⁷³. The method uses this subset to infer the proportion of
364 positive examples in the unlabeled sample.

- 365 • *Oracle*: Uses the true label y to estimate $p(y = 1|x)$. Importantly, this method cannot
366 actually be applied in real data since y is unobserved, but it represents an upper bound on
367 performance.

368 **S1 Related Work**

369 Because medical underdiagnosis is so ubiquitous, past work in both epidemiology and machine
370 learning has attempted to model and correct for it.

371 **Epidemiology** Numerous works in epidemiology address prevalence estimation in the context
372 of untrustworthy diagnostic tests⁷⁴ (a type of ascertainment bias, where diagnostic tests do not
373 reliably distinguish positive and negative cases⁷⁵). Early work characterized the impact of test
374 sensitivity, test specificity, and underlying disease prevalence on the accuracy of relative preva-
375 lence estimates^{14,76–80}, ultimately developing methods to adjust relative risk estimates given test
376 characteristics^{81–84}. The field naturally moved to consider the utility of tests with unknown speci-
377 ficity and sensitivity, and proposed methods to infer these test characteristics. Common approaches
378 include using external information (for example, ground truth annotations^{8–12}, multiple tests^{13–15},
379 or informative priors¹⁶). However, this type of information is frequently unavailable for underre-
380 ported medical conditions. We often have no access to ground truth, only a single diagnosis per
381 patient, and no notion of how accurate that diagnosis truly is.

382 **Machine Learning** The machine learning literature has also modeled underdiagnosis using the
383 positive-unlabeled (PU) learning framework, which assumes that only some positive cases are
384 correctly labeled as positive, and the unlabeled examples consist of both true negatives and unlabeled true positives. A key result in PU learning proves that without further assumptions — e.g.,
385 about the structure of the positive and negative distributions — it is impossible to estimate the
386 prevalence of an underreported condition⁸⁵. Many PU learning methods consequently introduce
387 assumptions about the structure of the positive and negative distributions in order to recover the
388 prevalence, including complete separability, positive subdomain^{56,57,86–88}, positive function^{61,72,73},
389 and irreducibility^{58,89}. All of these conditions represent different ways of encoding the basic as-
390 sumption that the negative distribution does not fully contain the positive distribution: in other
391 words, that there is a region of the feature space where cases are certain to be true positives.
392 However, this is a restrictive assumption which, while potentially suitable in other PU settings, is
393 unlikely to hold in health data¹⁷ because it is rare that a set of symptoms corresponds to a positive
394 diagnosis with 100% certainty. This is especially true in women’s health, where symptoms are fre-
395 quently not specific to a particular condition (for example, menstrual irregularities could suggest a
396 number of underlying conditions, rather than just one).
397

ICD Code	ICD Code Description
2724	Other and unspecified hyperlipidemia
2859	Anemia, unspecified
30000	Anxiety state, unspecified
412	Old myocardial infarction
41401	Coronary atherosclerosis of native coronary artery
42731	Atrial fibrillation
496	Chronic airway obstruction, not elsewhere class...
5849	Acute kidney failure, unspecified
E039	Hypothyroidism, unspecified
E669	Obesity, unspecified
F419	Anxiety disorder, unspecified
I10	Essential (primary) hypertension
I4891	Unspecified atrial fibrillation
N179	Acute kidney failure, unspecified
V5861	Long-term (current) use of anticoagulants
V5866	Long-term (current) use of aspirin
Y929	Unspecified place or not applicable
Z7901	Long term (current) use of anticoagulants
Z794	Long term (current) use of insulin

Table S1: Common Suspicious Symptoms. Suspicious symptoms for the semi-synthetic dataset created using common symptoms. We select these symptoms randomly from the 50 most common ICD codes in MIMIC-IV.

ICD Code	ICD Code Description
20410	Chronic lymphoid leukemia, without mention of ...
41402	Coronary atherosclerosis of autologous vein by...
43310	Occlusion and stenosis of carotid artery witho...
53085	Barrett's esophagus
5569	Ulcerative colitis, unspecified
8730	Open wound of scalp, without mention of compli...
K2270	Barrett's esophagus without dysplasia
V1051	Personal history of malignant neoplasm of bladder
V422	Heart valve replaced by transplant
V4581	Aortocoronary bypass status

Table S2: High Relative Prevalence Suspicious Symptoms. Diagnoses that are disproportionately more common among white patients. We filter out codes that appear fewer than 50 times in either group (white or Black patients). We then rank all codes by their prevalence among white patients divided by prevalence among Black patients. We then select the top 10 ICD codes. Our motivation is to ensure PURPLE recovers accurate relative prevalence estimates when the suspicious symptoms are highly correlated with the group variable, and when the true relative prevalence estimate is far from 1.

ICD Code	ICD Code Description
N80	Endometriosis
N800	Endometriosis of uterus
N801	Endometriosis of ovary
N802	Endometriosis of fallopian tube
N803	Endometriosis of pelvic peritoneum
N804	Endometriosis of rectovaginal septum and vagina
N805	Endometriosis of intestine
N806	Endometriosis in cutaneous scar
N808	Other endometriosis
N809	Endometriosis, unspecified
6179	Endometriosis, site unspecified

Table S3: Endometriosis Diagnoses. Diagnoses used to identify endometriosis cases. We use all symptoms containing reference to endometriosis, and identify these by filtering for ICD codes whose long descriptions (as described by MIMIC-IV¹) contain the word “endometriosis”.

ICD Code	ICD Code Description
33819	Other acute pain
5951	Chronic interstitial cystitis
6205	Torsion of ovary, ovarian pedicle, or fallopian...
6260	Absence of menstruation
78902	Abdominal pain, left upper quadrant
78904	Abdominal pain, left lower quadrant
78905	Abdominal pain, periumbilic
7891	Hepatomegaly
C561	Malignant neoplasm of right ovary
D251	Intramural leiomyoma of uterus
D252	Subserosal leiomyoma of uterus
D259	Leiomyoma of uterus, unspecified
D270	Benign neoplasm of right ovary
E43	Unspecified severe protein-calorie malnutrition
F911	Conduct disorder, childhood-onset type
G8921	Chronic pain due to trauma
K661	Hemoperitoneum
N739	Female pelvic inflammatory disease, unspecified
N952	Postmenopausal atrophic vaginitis
O210	Mild hyperemesis gravidarum
O2341	Unspecified infection of urinary tract in pregn...
O26891	Other specified pregnancy related conditions, f...
Q600	Renal agenesis, unilateral
R1310	Dysphagia, unspecified
R17	Unspecified jaundice

Table S4: Correlated Suspicious Symptoms. Suspicious symptoms for the semi-synthetic dataset created using symptoms correlated with endometriosis. We select the 25 ICD codes with the highest relative proportion among endometriosis patients (where endometriosis patients are identified as patients receiving any ICD code appearing in Table S3).

ICD Code	ICD Code Description
7842	Swelling, mass, or lump in head and neck
9100	Abrasion or friction burn of face, neck, and sc...
920	Contusion of face, scalp, and neck except eye(s)
95901	Head injury, unspecified
S0003XA	Contusion of scalp, initial encounter
S0011XA	Contusion of right eyelid and periocular area, ...
S0012XA	Contusion of left eyelid and periocular area, i...
S0990XA	Unspecified injury of head, initial encounter

Table S5: Recognized Suspicious Symptoms. Diagnoses associated with intimate partner violence. We first identify all ICD codes that refer to head, neck, and face injuries (100 ICD codes). We filter out codes that appear fewer than 10 times as a part of dataset preprocessing (§M2.2), which leaves the 8 codes listed here.

ICD Code	ICD Code Description
E9672	Perpetrator of child and adult abuse, by mothe...
E9673	Perpetrator of child and adult abuse, by spous...
E9671	Perpetrator of child and adult abuse, by other...
E9670	Perpetrator of child and adult abuse, by fathe...
E9679	Perpetrator of child and adult abuse, by unspe...
V6111	Counseling for victim of spousal and partner a...
99581	Adult physical abuse
99585	Other adult abuse and neglect
T7411XA	Adult physical abuse, confirmed, initial encou...
T7411XD	Adult physical abuse, confirmed, subsequent en...
T7411XS	Adult physical abuse, confirmed, sequela
99580	Adult maltreatment, unspecified
T7611	Adult physical abuse, suspected
T7611XA	Adult physical abuse, suspected, initial encou...
T7611XD	Adult physical abuse, suspected, subsequent en...
T7611XS	Adult physical abuse, suspected, sequela
T7611XA	Adult physical abuse, suspected, initial encou...
T7611XD	Adult physical abuse, suspected, subsequent en...
T7611XS	Adult physical abuse, suspected, sequela
Y070	Spouse or partner, perpetrator of maltreatment...
Y0701	Husband, perpetrator of maltreatment and neglect
Y0702	Wife, perpetrator of maltreatment and neglect
Y0703	Male partner, perpetrator of maltreatment and ...
Y0704	Female partner, perpetrator of maltreatment an...
Y079	Unspecified perpetrator of maltreatment and ne...

Table S6: IPV Diagnoses. Diagnoses used to identify positive intimate partner violence cases. We use symptoms collected from prior work, including surveys used to study the prevalence of intimate partner violence^{7,18,90,91}, in addition to manual examination of the ICD-10 and ICD-9 codebook.

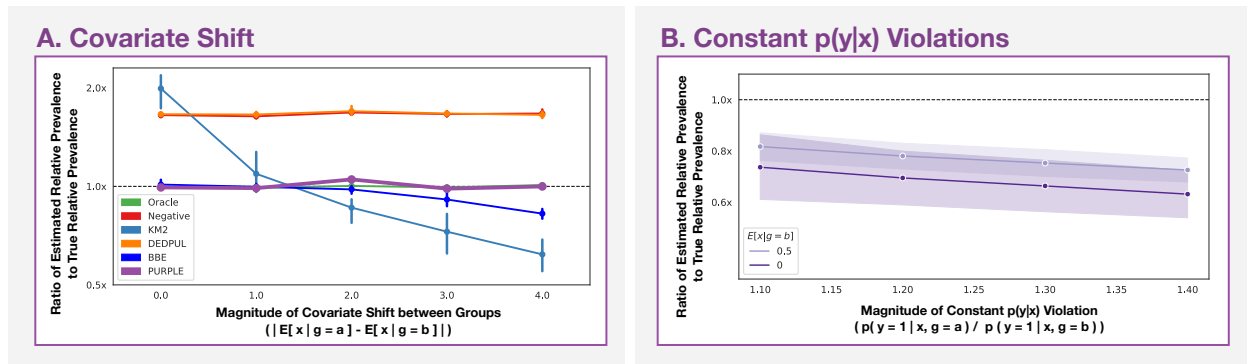


Figure S1: Robustness checks on synthetic data. A) PURPLE is robust to differences in group-specific covariate distributions. PURPLE produces consistently accurate relative prevalence estimates across simulations with increasingly different groups, where we simulate group differences by altering the magnitude of the difference between group means ($|E[x|g=a] - E[x|g=b]|$). **B) PURPLE still yields useful lower bounds on prevalence disparities even if $p(y=1|x)$ varies between groups.** Under a plausible violation of the assumption that $p(y=1|x)$ remains constant across groups, PURPLE can lower-bound the true relative prevalence. Specifically, if the same symptoms correspond to a higher likelihood of a condition in the group with a higher overall prevalence (i.e., $p(y=1|x, g=a) > p(y=1|x, g=b)$ if $p(y=1|g=a) > p(y=1|g=b)$), PURPLE produces an underestimate of the true relative prevalence. Different shades of purple correspond to different magnitudes of covariate shift between groups.

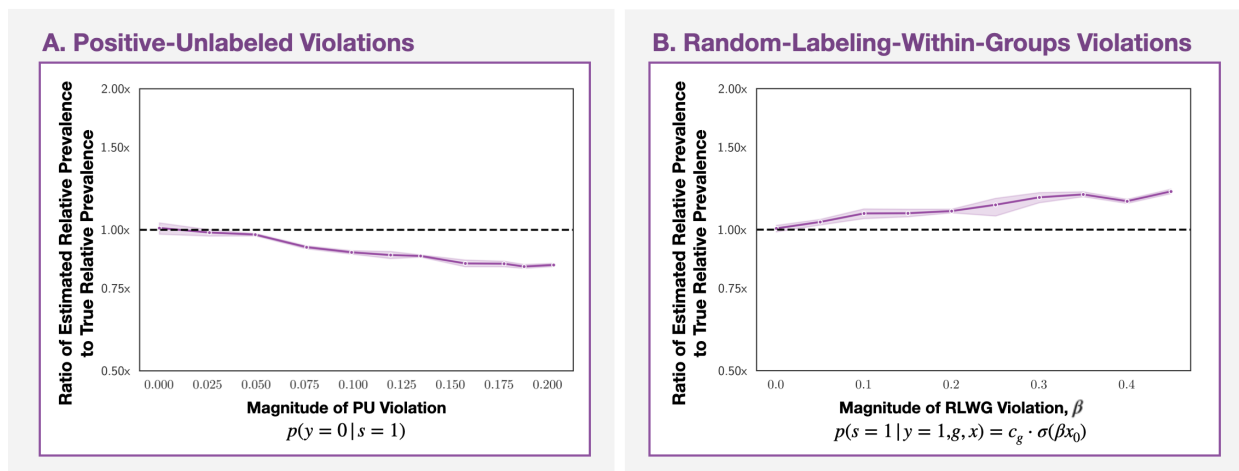


Figure S2: Robustness to violations of assumptions on synthetic data. A) Effects of violations of positive-unlabeled assumption. We plot the behavior of PURPLE as we increase the percentage of false positives present in the “positive sample”, or all examples where $s = 1$. As expected, PURPLE recovers the relative prevalence exactly when there are no false positives in the positive sample, and performance degrades as this percentage increases. **B) Effects of violations of the random-diagnosis-within-groups assumption.** As the magnitude of β increases, the diagnosis probability becomes more correlated with feature X_0 , thereby violating the random-diagnosis-within-groups assumption. As expected, these violations, produce larger errors in PURPLE’s estimates of the relative prevalence. We illustrate the impact of these violations to characterize PURPLE’s behavior under violations of the central assumptions and provide checks for whether these assumptions are collectively violated in Sec. M1.5.

Relative Prevalence of Intimate Partner Violence

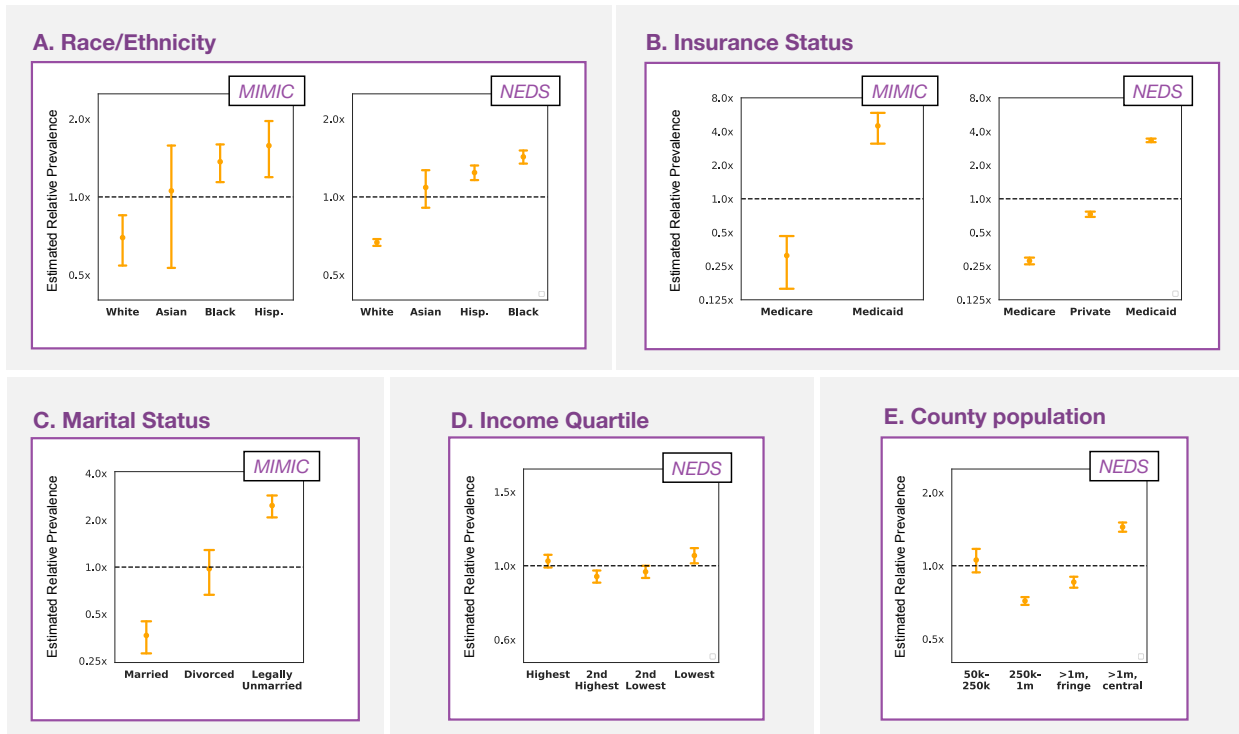


Figure S3: Comparing PURPLE to relative prevalence estimates which do not correct for underdiagnosis. We compare PURPLE’s relative prevalence estimates to relative prevalence estimates based on $p(s = 1|g)$ across groups — which simply uses observed diagnoses s , and does not correct for underdiagnosis. Orderings across groups for race, insurance status, and marital status are qualitatively similar for both methods. When we look at intimate partner violence prevalence across income quartiles, however, we see that PURPLE’s relative prevalence estimates agree more closely with prior work, which has found that rates of intimate partner violence decrease with income. Further, PURPLE infers that intimate partner violence is underdiagnosed among women in the lowest income quartile, which is supported by prior work on underdiagnosis among low-income patients. In contrast, the estimates which do not correct for underdiagnosis do not reveal a monotonic trend, and are harder to reconcile with past work.

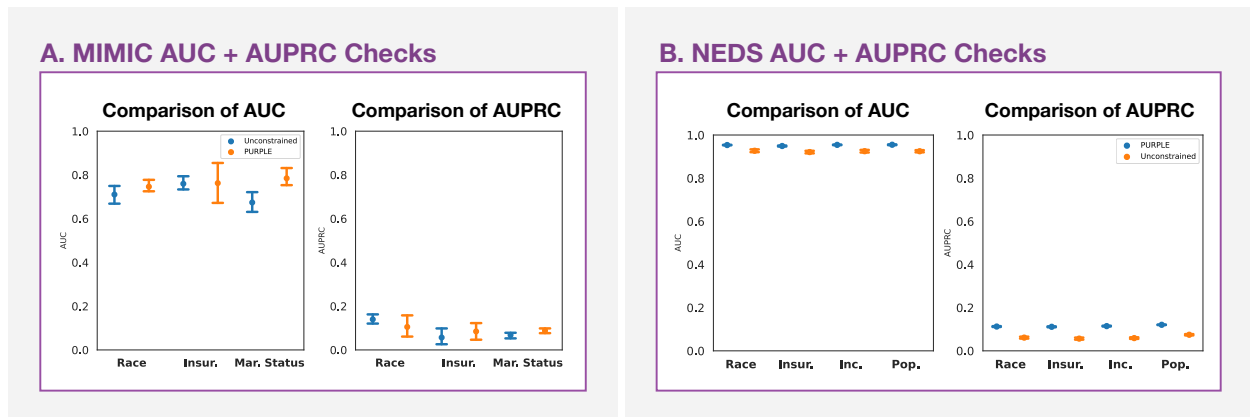


Figure S4: Model check: Comparison of PURPLE and unconstrained model on MIMIC-IV data (A) and NEDS data (B). The unconstrained model is a model with interactions between group status and features, allowing it to learn different likelihood functions $p(y = 1|x)$ for each group, in contrast to PURPLE, which assumes that the likelihood function remains constant across groups. We report results of the unconstrained model for each demographic category individually because each category corresponds to different subsets of patients (for example, the insurance category contains patients who are on Medicare or Medicaid, which filters out patients who are not on either). AUCs and AUPRCs of PURPLE are similar to the unconstrained model for all demographic categories and both datasets, indicating that PURPLE’s restriction in model form does not harm performance. (In some cases, PURPLE actually does slightly better than the unconstrained model, likely indicating that the interaction terms the unconstrained model has access to provide noise but not signal, making it more vulnerable to overfitting).

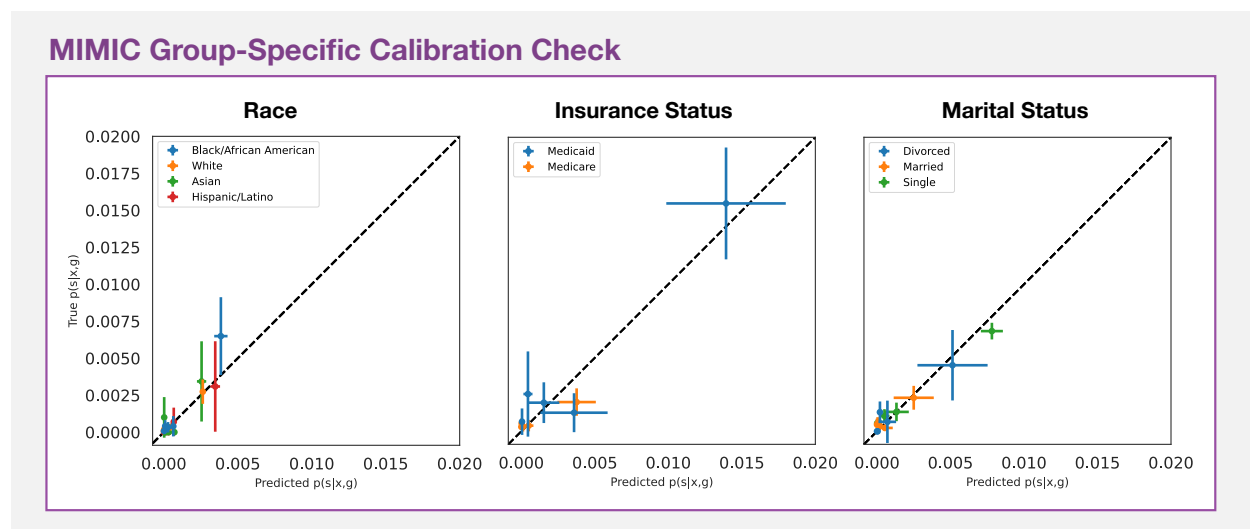


Figure S5: Model check: Group-specific calibration in MIMIC-IV data. PURPLE outputs calibrated probabilities across subgroups. We bin predictions into quintiles and plot the means of $\hat{p}(s = 1|x, g)$ and $p(s = 1|x, g)$ over 5 randomized dataset splits; errorbars show standard deviations across the 5 splits. The width of the error bars is due to the small number of positive examples in the intimate partner violence data. To ensure our calibration estimates are not overly noisy, in this analysis only we omit groups with fewer than 500 health records in the test set (e.g., Hispanic patients).

NEDS Group-Specific Calibration Check

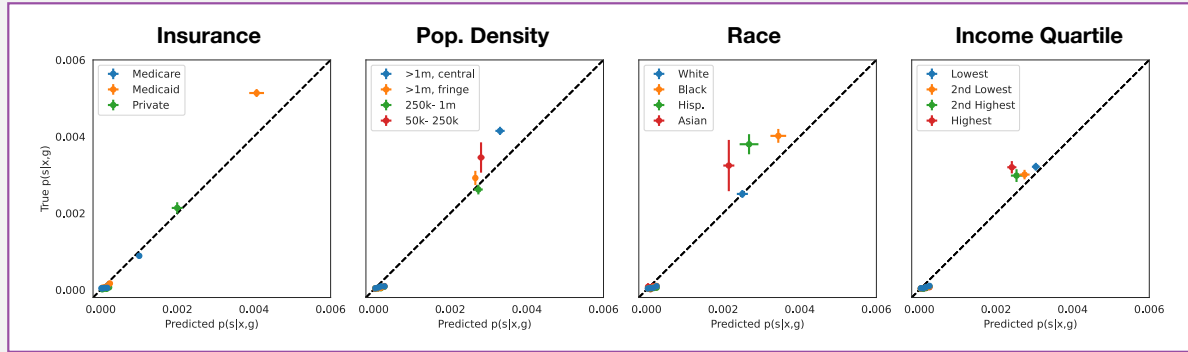


Figure S6: Group-specific calibration in NEDS. PURPLE is well-calibrated across subgroups. We bin predictions on the test set into quintiles and compare the average predicted probability of diagnosis ($\hat{p}(s = 1|x, g)$, horizontal axis) and the true probability of diagnosis ($p(s = 1|x, g)$, vertical axis) within each bin. We produce error bars, as before, by plotting the standard deviation of both $\hat{p}(s = 1|x, g)$ and $p(s = 1|x, g)$ for each bin across 5 randomized test sets.